2016

Safety evaluation of low level light therapy on cancer cells

BOSTON UNIVERSITY

SCHOOL OF MEDICINE

Thesis

SAFETY EVALUATION OF LOW LEVEL LIGHT THERAPY ON CANCER CELLS

by

ANDREW S. JEONG

B.A., Johns Hopkins University, 2010

Submitted in partial fulfillment of the

requirements for the degree of

Master of Arts

2016

Approved by

First Reader

James F. Head, Ph.D.
Professor of Physiology and Biophysics

Second Reader

Mei X. Wu, MD, Ph.D.
Associate Professor of Dermatology
Harvard Medical School

ACKNOWLEDGEMENTS

I would like to sincerely thank Dr. Mei X. Wu, Dr. Tingting Dong, and everyone else in the lab who provided me with gracious support throughout my time working on my thesis. I am grateful for their contributions in helping me in completing the thesis.

SAFETY EVALUATION OF LOW LEVEL LIGHT THERAPY

ON CANCER CELLS

ANDREW S. JEONG

ABSTRACT

Objective: Low level light therapy (LLLT) is being widely used in wound healing and pain relief, and its use is expected to be expanded rapidly to treatment of other disorders as well in a foreseeable future. However, before its expansion, the fear that LLLT could initiate or promote metastasis must be addressed thoroughly. As an initial effort towards this end, the current study evaluates the safety of LLLT in vitro using two different human cancer cell lines (Michigan Cancer Foundation-7 (MCF-7) and Jurkat E6-1) by determining the viability of cells after low level light (LLL) application while treatment under anti-cancer chemotherapeutic drugs (5-fluorouracil (5-FU) and cisplatin) separately on each cell line.

Methods: Two human cancer cell lines (MCF-7 and Jurkat E6-1) were cultured throughout the experiments. Two different anti-cancer chemotherapeutic drugs (5-FU and cisplatin) were used to treat both cell lines. The half maximal inhibitory concentration (IC_{50}) of each drug on each cell line was determined by treating each cell line with varying concentrations of each drug. A total of 3 or 4 trials were done for each cell line with each drug, and the range of concentration was narrowed closer to the IC_{50} value at each successive trial. Once the IC_{50} concentrations were determined, each cell line was treated with 808 nm LLL at varying energy densities in a single dose using a light emitting diode (LED) source both in the absence and the presence of each drug at one

IC_{50}. A total of 3 or 5 trials were done for each cell line with each drug, and for each trial, six different energy densities ranging from 0 J/cm^2 (control) to 10 J/cm^2 were applied. The energy densities were varied for each trial with control always being used. After application of LLL, the viability of cells was determined, and three different 1-way ANOVA (Analysis of Variance) analyses were done to compare the viability of cells at each energy density to that of control.

Results: The IC_{50} of 5-FU in MCF-7 and Jurkat E6-1 cells was determined as 70 μM and 20 μM respectively. The IC_{50} of cisplatin in MCF-7 and Jurkat E6-1 cells was determined as 17 μM and 7 μM respectively. No significant difference ($P > 0.05$) in the viability of MCF-7 cells was observed between each group treated with different energy density of LLL and control group (0 J/cm^2) both in the absence and the presence of 5-FU at IC_{50} (70 μM). No significant difference ($P > 0.05$) in the viability of MCF-7 cells was observed between each group treated with different energy density of LLL and control group (0 J/cm^2) both in the absence and the presence of cisplatin at IC_{50} (17 μM). No significant difference ($P > 0.05$) in the viability of Jurkat E6-1 cells was observed between each group treated with different energy density of LLL and control group (0 J/cm^2) both in the absence and the presence of 5-FU at IC_{50} (20 μM). However, a significant increase ($0.01 < P < 0.05$) in the viability of cells was observed when treating Jurkat E6-1 cells with 10 J/cm^2 of LLL in the presence of cisplatin at IC_{50} (7 μM) compared to control group (0 J/cm^2). Except for the comparison mentioned previously, no significant difference in the viability of Jurkat E6-1 cells was observed between each group treated with different energy density of LLL and control group (0 J/cm^2) both in the absence and

the presence of cisplatin at IC_{50} (7 μM). No definite trend in the viability of cells was observed with increasing energy density of LLL for each cell line either in the absence of the presence of each drug at IC_{50}.

Conclusions: The application of LLL at 808 nm with energy densities ranging from 0.1 J/cm^2 to 10 J/cm^2 under an LED source did not induce cell proliferation or death compared to control (0 J/cm^2) for each cell line in the absence or the presence of each drug, and no definite trend was observed with increasing energy density. The study suggests that LLLT at these parameters may be safe to use on cancer patients, but further studies on different cancer cell lines and animal models with different parameters (wavelength, energy density, dosage) of LLL are warranted.

TABLE OF CONTENTS

LIST OF TABLES

LIST OF FIGURES

ABBREVIATIONS

ANOVA	Analysis of Variance
AP-1	Activator Protein-1
ATCC	American Type Culture Collection
ATF	Activating Transcription Factor
ATP	Adenosine Triphosphate
bFGF	basic Fibroblast Growth Factor
cAMP	Cyclic Adenosine Monophosphate
CCK-8	Cell Counting Kit-8
cDNA	Complementary Deoxyribonucleic Acid
CREB	cAMP-Response Element-Binding protein
DNA	Deoxyribonucleic Acid
dTTP	Deoxythymidine Triphosphate
H.EP.2	Human Epithelial type 2
HIF	Hypoxia-inducible Factor
HIF-1α	Hypoxia-inducible Factor-1α
IC_{50}	The half maximal inhibitory concentration
IL-6	Interleukin-6
JAK	Janus family of protein tyrosine kinase
LED	Light Emitting Diode
LLL	Low Level Light

LLLT	Low Level Light Therapy
MCF-7	Michigan Cancer Foundation-7
MMP	Matrix Metalloproteinase
MMP-1	Matrix Metalloproteinase-1
MTT	Microculture Tetrazolium
NF-kB	Nuclear Factor kappa-light-chain-enhancer of activated B cells protein
NIR	Near-infra Red
NO	Nitric Oxide
NS	No Significance
PDGF	Platelet-derived Growth Factor
PBS	Phosphate-buffered Saline
Ref-1	Redox factor-1
ROS	Reactive Oxygen Species
RPMI-1640	Roswell Park Memorial Institute-1640
TC	Tissue Culture
TGF-β	Transforming Growth Factor-β
TGF-β1	Transforming Growth Factor-β1
TIMP	Tissue Inhibitor of Metalloproteinase
UV	Ultra Violet
WST-8	Water Soluble Tetrazolium-8
5-FU	5-Fluorouracil

INTRODUCTION

LLLT also known as low level laser therapy is being used increasingly for the treatment of multitude of conditions in medicine. At first, it has been used mainly for wound healing and relief of pain and inflammation, but in recent years, its use in treatment has become broadened to a variety of conditions such as stroke, myocardial infarction, arthritis, musculoskeletal disorders, degenerative brain disorders, dental pathologies, and skin diseases etc. LLLT commonly uses red and near infra-red light which are produced by laser and LEDs (Myakishev-Rempel, et al., 2012). As illustrated in Figure 1, laser is a coherent light source in which the light waves are in-phase and monochromatic. Unlike sun light which consists of multiple wavelengths with rays scattering in all directions, laser light consists of a single wavelength, with its rays stacked to each other side by side, focusing in a narrow beam. LED is non-coherent light sources consisting of filtered lamps. Although monochromatic, the waves are out-of-phase. LED devices produce light with wavelengths similar to those of lasers, but they are less monochromatic in that they have broader output peaks, and lack the coherence that laser has.

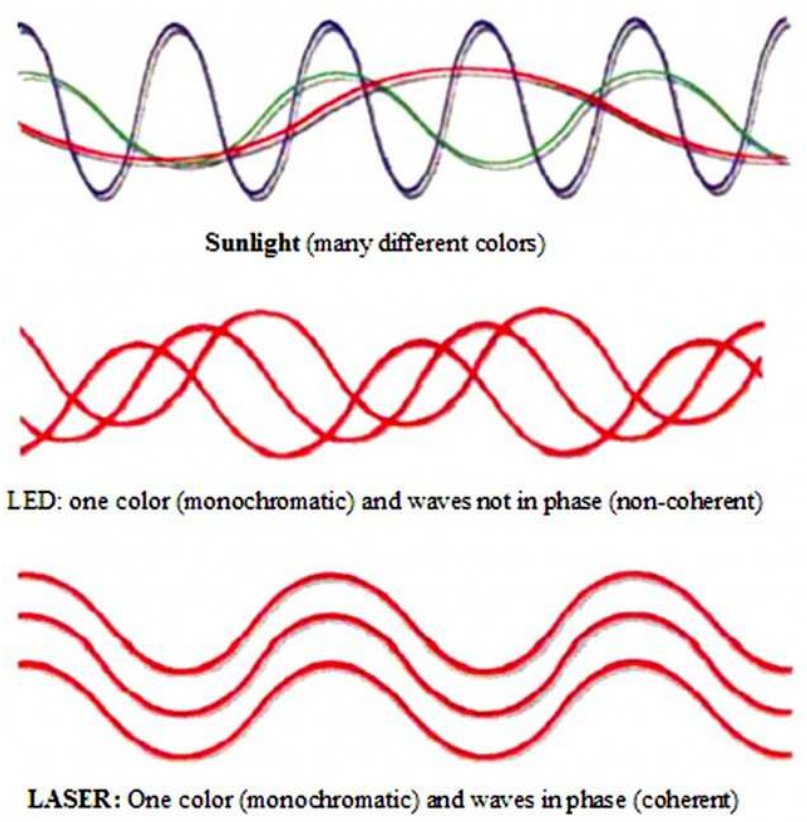

Figure 1. The difference between sunlight, LED light and laser light. Abbreviation: LED: Light-Emitting Diode (multichromatic, sunlight, monochromatic and coherent light, 2011).

LLLT utilizes either laser or LEDs or a combination of both (What is LLLT? - THOR Laser, 2015). It is considered "low level" or "low power" since the energy or power densities used are low compared to other forms of laser that are used for ablation, cutting, and thermally coagulating tissue (Hamblin, 2008). Its wavelength typically ranges from 600 nm to 1000 nm, and light emitting devices typically deliver from 10 mW to 500 mW, and the power density typically ranges from 0.005 W/cm^2 to 5 W/cm^2 (What is LLLT? - THOR Laser, 2015). The medical applications of LLLT has been progressively broadened, however, the biochemical mechanisms by which tissues respond to LLL, and the underlying positive effects are incompletely understood. Also,

the complexity of rationally choosing amongst a large number of parameters such as energy density, wavelength, fluence, exposure time, and pulse structure has led to the publication of numerous studies revealing conflicting outcomes regarding its safety and effectiveness. In particular, a biphasic dose response has been frequently reported where low levels of light have a much better effect than higher levels (Hamblin, 2008). This demonstrates a clear need to elucidate the proper usage of parameters in terms of its safety and effectiveness, and this study aims to evaluate the safety of LLLT on two different cancer cell lines in vitro.

History of Light Therapy

Light therapy is one of the oldest therapeutic methods used by humans historically as solar therapy by Egyptians and later as ultra violet (UV) therapy for which Nils Finsen won the Nobel prize in 1904. In 1967, Endre Mester in Semmelweis University, Budapest, Hungary, tested if laser radiation might cause cancer in mice. He shaved the dorsal hair and divided them into two groups, then applied laser with a low powered ruby laser (694 nm) to one group. The mice from the laser-treated group did not get cancer, and surprisingly, the hair on the laser-treated group grew back more quickly than the untreated group. This was the first demonstration of "laser biostimulation." Since then, medical treatment with coherent light sources such as lasers or non-coherent light sources such as LEDs became more prevalent, and currently, LLLT is practiced in variety of medical fields in treating many different conditions. The question is no longer whether or not light has biological effects, but rather how energy from lasers and LEDs work at the

cellular level and in the organism as a whole, and what are the optimal light parameters for different uses of these light sources (Hamblin, 2008).

Biphasic Dose Response

Through clinical studies and studies involving cell culture and animal models, it has been found that there exists an optimal dose of light for any particular application, and doses lower than this optimal value, or more significantly, higher than the optimal value would decrease the therapeutic outcome. In fact, for higher doses of light, a negative outcome may even result. Evidence suggests that energy density is a key biological parameter for the safety and the effectiveness of LLLT, and it may operate with thresholds in which there exists a point where LLLT is too weak to have any effect or so strong to cause over-stimulation (Hamblin, 2008).

Biochemical Mechanisms

The quantum mechanical theory states that light energy is composed of photons or discrete packets of electromagnetic energy. The energy of an individual photon depends only on the wavelength. Therefore, the energy of a dose of light depends only on the number of photons and on their wavelength. Photons that are delivered into tissue can be either absorbed or scattered. Scattered photons will eventually be absorbed or will diffusely reflect off from the tissue. The photons that are absorbed interact with an organic molecule or chromophore within the tissue. According to the first law of thermodynamics, the energy delivered to the tissue must be conserved, and three possible pathways exist to account for what happens to the delivered light energy within the tissue. The pathways are internal conversion, fluorescence, and a number of processes broadly

grouped under photochemistry including energy transfer, electron transfer, and dissociation of a non-covalently bound ligand from a binding site on a metal-containing cofactor in an enzyme. These proposed pathways could be the mechanisms of how LLLT induces changes in treating conditions that are part of three main areas of medicine where LLLT has been broadly used as demonstrated in Figure 2. These are wound healing, tissue repair, and prevention of tissue death; relief of inflammation in chronic diseases and injuries with its associated pain and edema; relief of neurogenic pain and neurological problems (Hamblin, 2008). Also, in vitro, animal, and clinical studies revealed that LLLT can prevent cell apoptosis, and enhance cell proliferation, migration, and adhesion as demonstrated in Figure 3.

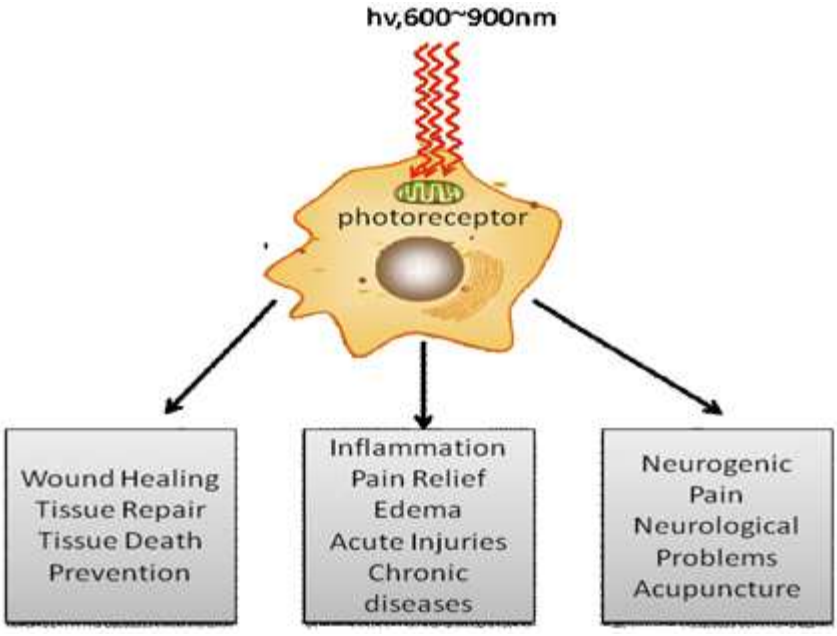

Figure 2. Schematic representation of the main applications of LLLT. hv: light energy where h = Planck's constant (~6.626 x 10^{-34} m^2kg/s) and v = frequency. Abbreviation: LLLT: Low Level Light Therapy (Huang, Hamblin, & Chen, 2009).

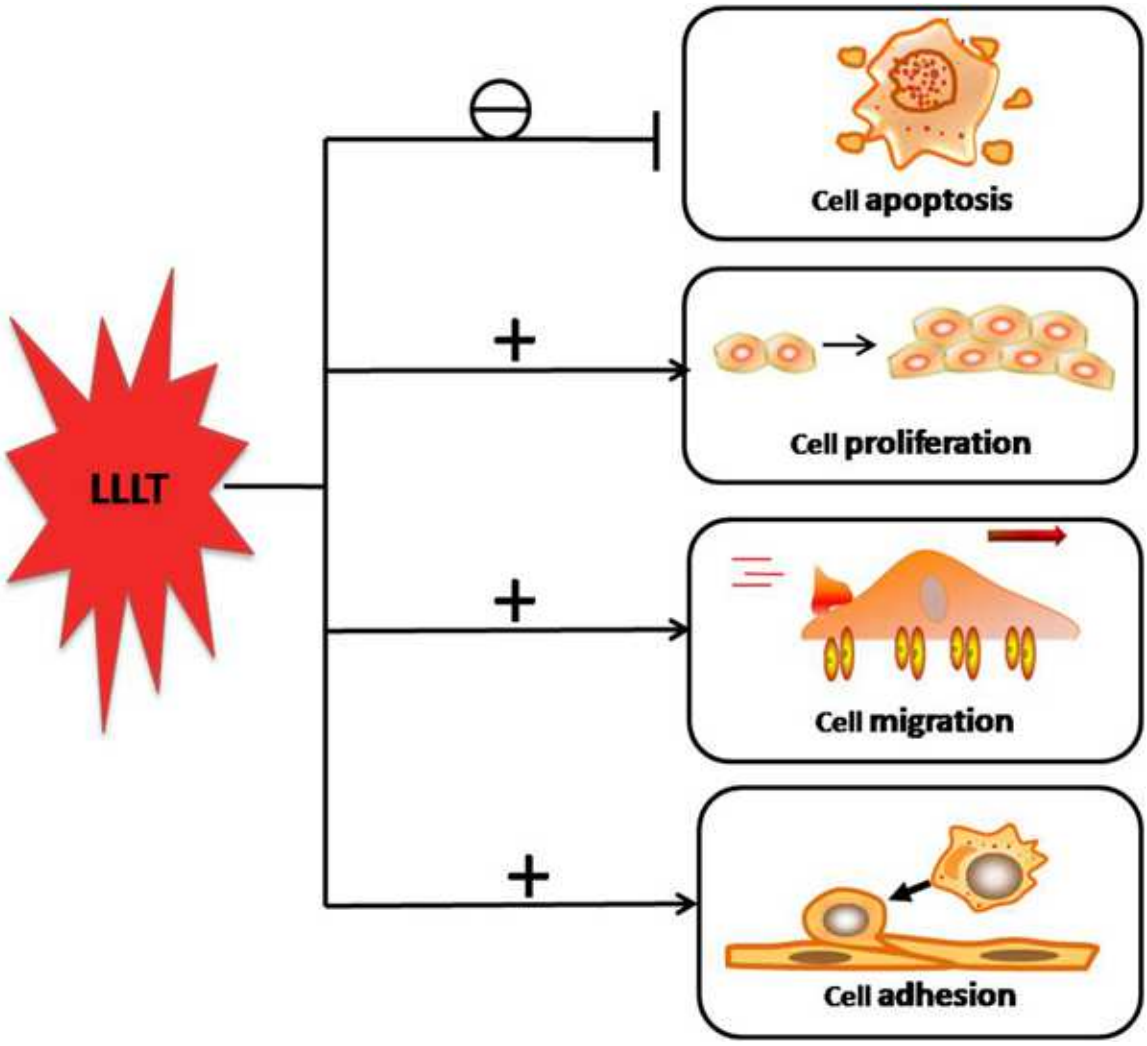

Figure 3. Cellular effects of LLLT. Abbreviation: LLLT: Low Level Light Therapy (Huang, Hamblin, & Chen, 2009).

The suggested mechanism of LLLT at the cellular level was based on the absorption of monochromatic visible and near-infra red (NIR) radiation by components of the cellular respiratory chain. It was proposed that cytochrome c oxidase which contains two iron centers (haem a and haem a_3), and two copper centers (CuA and CuB), is the primary photoacceptor for the red-NIR range in mammalian cells (Hamblin, 2008). When the effect of He-Ne laser illumination (632.8 nm) on the purified cytochrome c

oxidase was examined, there was an increased oxidation of cytochrome c and increased electron transfer (Pastore, Greco, & Passarella, 2000). Also, increased activity of catalase was observed after He-Ne laser illumination (Artyukhov, Basharina, Pantak, & Sveklo, 2000). The absorption of photons by molecules leads to electronically excited states, and consequently may lead to an acceleration of electron transfer reactions. Increase in electron transport leads to an increase in the production of adenosine triphosphate (ATP), which in turn leads to an increase in proton gradient. The increased proton gradient leads to an increase in activity of Na^+/H^+ and Ca^{2+}/Na^+ antiporters, and of all the ATP-driven carriers for ions including Na^+/K^+ ATPase and Ca^{2+} pumps (Hamblin, 2008).

Ability of light to influence the localized production or release of nitric oxide (NO) was demonstrated by many studies including Guzzardella et al and Tuby et al (Guzzardella, Fini, Torricelli, Giavaresi, & Giardino, 2002), (Tuby, Maltz, & Oron, 2006). This signifies that properly designed illumination devices may be effective therapeutic agents for patients who would benefit from increased localized NO availability. The activity of cytochrome c oxidase is inhibited by NO, and this inhibition of mitochondrial respiration by NO can be explained by a direct competition between NO and O_2 for the reduced binuclear center CuB/a_3 of cytochrome c oxidase, and is reversible. It was proposed that laser irradiation could reverse the inhibition of cytochrome c oxidase by NO by photodissociating NO from its binding sites, both in isolated mitochondria and in whole cells. The dissociation of NO from cytochrome c oxidase will thus increase the respiration rate and the production of ATP. The other proposed mechanism was the "redox properties alteration hypothesis," which states that the alteration of mitochondrial

metabolism and the activation of the respiratory chain by illumination would also increase the production of superoxide anions (Hamblin, 2008).

Changes in cellular redox state induce the activation of numerous intracellular signaling pathways, and these cytosolic responses in turn induce transcriptional changes. Several transcription factors are regulated by these changes, and they are redox factor-1 (Ref-1)-dependent activator protein-1 (AP-1), nuclear factor kappa-light-chain-enhancer of activated B cells protein (NF-kB), p53, activating transcription factor/cyclic adenosine monophosphate (cAMP)-response element-binding protein (ATF/CREB), hypoxia-inducible factor-1α (HIF-1α), and hypoxia-inducible factor (HIF)-like factor etc. Figure 3 illustrates the effect of redox-sensitive transcription factors activated after application of NIR in causing the transcription of gene products that eventually lead to cell proliferation, growth factors production, extracellular matrix deposition, and cell motility etc. As a rule, the oxidized form of redox-dependent transcription factors have low deoxyribonucleic acid (DNA)-binding activity. Ref-1 is an important factor for the specific reduction of these transcription factors. However, it was also shown that low levels of oxidants appear to stimulate proliferation and differentiation of some type of cells. It was proposed that LLLT produces a shift in overall cell redox potential in the direction of greater oxidation. Different cells at a range of growth conditions have distinct redox states. Therefore, the effects of LLLT can vary considerably. Cells being initially at a more reduced state like primary cells have high potential to respond to LLLT, while cells at the optimal redox state like cancer cells respond weakly or do not respond to treatment with light (Hamblin, 2008).

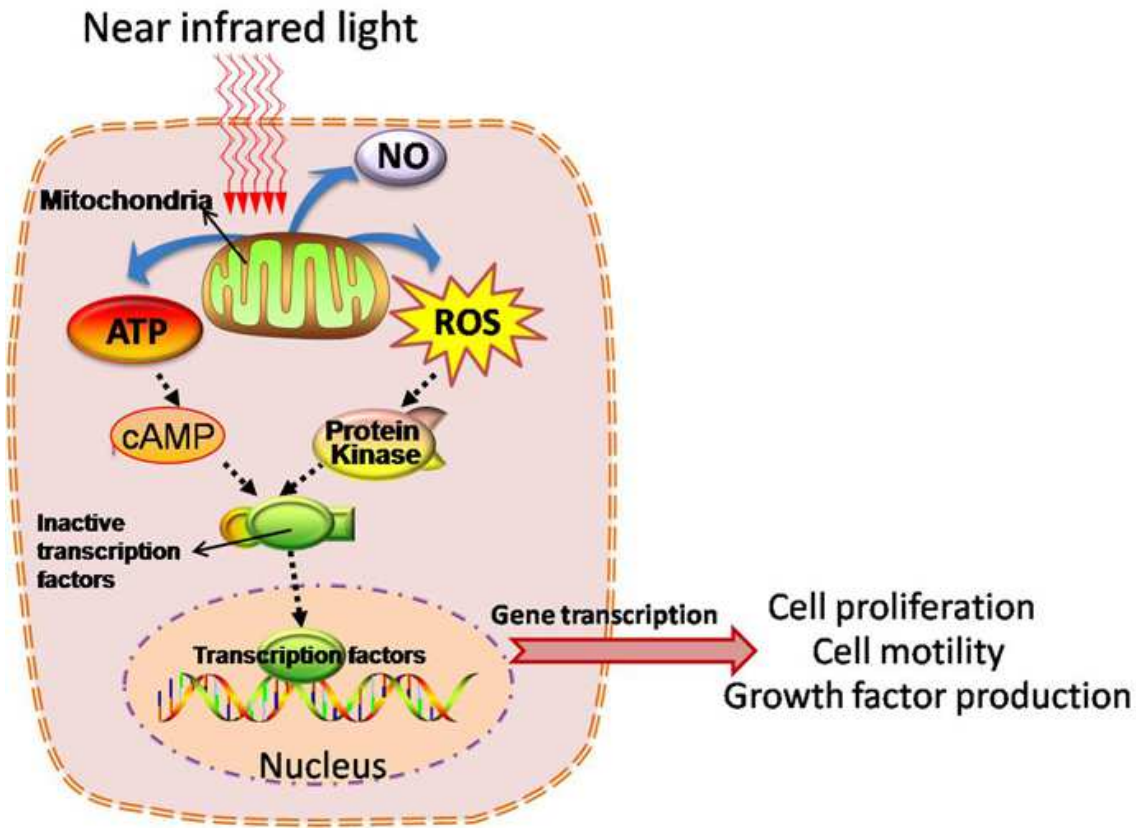

Figure 4. Cell signaling mechanisms induced by NIR. Abbreviations: ATP: Adenosine Triphosphate, cAMP: cyclic Adenosine Monophosphate, NIR: Near-infra Red, NO: Nitric Oxide, ROS: Reactive Oxygen Species (Huang, Hamblin, & Chen, 2009).

Cellular Responses Observed in vitro after LLLT

The cellular responses observed in vitro after LLLT can be broadly classed under increases in metabolism, migration, proliferation, and increases in synthesis and secretion of various proteins. A study by Zhang et al. exposed normal human fibroblasts for 3 days to 0.88 J/cm^2 of 628 nm light from a light emitting diode. Gene expression profiles upon irradiation were examined using a complementary deoxyribonucleic acid (cDNA) microarray containing 9982 human genes, and 111 genes were found to be affected by light. All genes from the antioxidant related category and genes related to energy

metabolism and respiratory chain were upregulated. Most of the genes related to cell proliferation were upregulated as well. Amongst genes related to apoptosis and stress response, some genes such as Janus family of protein tyrosine kinase (JAK) binding protein were upregulated, and others such as caspase 6 and stress-induced phosphoprotein were downregulated. It was suggested that LLLT stimulated cell growth directly by regulating the expression of specific genes, as well as indirectly by regulating the expression of the genes related to DNA synthesis and repair, and cell metabolism (Zhang, et al., 2003).

The effects of LLLT on cell proliferation are debatable because studies have found both an increase and a decrease in proliferation of cells. Cell culture is an excellent method to assess both effects with varying doses of treatments. Red light is known to have a mitogenic effect based on its ability to activate cell division at certain spectral and dose ranges in vitro. A study by Pinheiro et al. assessed the effect of 635 nm and 670 nm laser irradiation of human epithelial type 2 (H.Ep.2) cells in vitro using microculture tetrazolium (MTT) assay. The cells were obtained from squamous cell carcinoma of the larynx and were routinely processed from defrost to the experimental condition. Twenty-four hours after transplantation the cells were irradiated with LLL with 635 nm or 670 nm doses ranging from 0.04 J/cm^2 to 0.48 J/cm^2 for seven consecutive days. The results showed that 635 nm laser light did not significantly stimulate the proliferation of H.Ep.2 cells at doses of 0.04 J/cm^2 to 0.48J/cm^2, however, 670 nm laser irradiation led to an increased cell proliferation when compared to both control and 635 nm irradiated cells. The best cell proliferation was found with 670 nm laser irradiated cultures exposed to

doses of 0.04 J/cm^2 to 0.48 J/cm2. Based on these results, both dose and wavelength are factors that may affect cell proliferation of H.Ep.2 cells (Pinheiro, et al., 2002).

There exist contradictory reports about low-intensity laser light-stimulated cell proliferation. A study by Moore et al. measured the proliferation of primary cell cultures after irradiation with varying laser wavelengths to determine the effect of wavelength on proliferation of cultured murine cells. Fibroblasts proliferated faster than endothelial cells in response to laser irradiation. Maximum cell proliferation occurred with 665 nm and 675 nm light, whereas 810 nm light was inhibitory to fibroblasts. These outcomes suggest that both wavelength and cell type influence the cell proliferation in response to low-intensity laser irradiation (Moore, Ridgway, Higbee, Howard, & Lucroy, 2005).

A study by El Batanouny investigated the mitogenic and genotoxic effects of He:Ne laser irradiation (632.8 nm) on human peripheral lymphocytes in vitro. In this study, buffy coat leukocytes were exposed to 10 mW He:Ne laser at energy densities of 1, 2, 3 and 5 J/cm^2. Cells were then cultured in media 199 without any supplementation for 24, 48, 72 and 96 hours adding cytochalasin B 24 hours before harvesting of cells. The results revealed that laser-induced lymphocytes proliferate throughout the four consecutive days post-laser irradiation. The difference in the frequency of micronuclei between pre- and post-laser irradiation indicates that a He:Ne laser at such energy densities 1, 2, 3 and 5 J/cm^2 does not induce micronucleus formation. These results shed some light on the mechanism encountered by lymphocytes in the process of He:Ne laser-induced biostimulation (El Batanouny, Korraa, & Fekry, 2002).

Safety of LLLT on Tissues Harboring Cancer

The use of LLLT in cancer patients, including the treatment of lymphedema or various unrelated comorbidities, has been withheld by practitioners because of the fear that LLLT might result in initiation or promotion of metastatic lesions or new primary tumors. Although it is unlikely that LLLT would directly induce de novo cancer development as there has been no scientific evidence that LLLT triggers DNA damage, its effects on cellular proliferation have been the empiric basis for withholding treatment in cancer patients. A study by Myakishev-Rempel et al. investigated whether LLLT would promote tumor growth when pre-existing malignancy is present. In this study, a standard SKH mouse nonmelanoma UV-induced skin cancer model was used after visible squamous cell carcinomas were present. The red light group received automated full body 670 nm LLLT delivered twice a day at 5 J/cm^2 using an LED source. The control group was handled similarly, but did not receive LLLT. Measurements on 330 tumors were conducted for 37 consecutive days, while the animals received daily LLLT. Daily tumor measurements demonstrated no measurable effect of LLLT on tumor growth, and the results suggest that LLLT at these parameters may be safe even when malignant lesions are present (Myakishev-Rempel, et al., 2012).

Conflicting outcomes were shown in other studies. One study demonstrated the acceleration of tumor growth by 633 nm laser irradiation at 3.5 J/cm^2 three times per week for 2 weeks in a model of human gastric adenocarcinoma transplanted into immunodeficient athymic nude mice. This suggests that LLLT is indeed capable of activating tumor growth under conditions that exclude immune resistance (Myakishev-

Rempel, et al., 2012). In another study, the irradiation of squamous cell carcinomas in the hamster cheek pouch with 660 nm light at 56 J/cm^2, a very high energy density and a 3 mm spot caused significant progression of the severity of squamous cell carcinomas as judged by histology (de C. Monteiro, et al., 2011).

Application of LLLT in Mucosal Healing and Skin

The effects of LLLT in mucosal healing in an acute colitis model in mice was demonstrated by a study by Zigmond et al., in which colitis was induced by dextran sodium sulfate in four blinded controlled studies. LLLT was applied to the colon utilizing a small diameter endoscope with an LED-based light source in several wavelengths including 440, 660, and 850 nm at 1 J/cm^2 and then 850 nm at several doses including 1, 0.5, 0.25, and 0.1 J/cm^2. LLLT was initiated 1 day prior to induction of colitis and went on for the 6 day induction period as well as for the following 3–10 days. Disease activity was scored endoscopically and histopathologically. The results showed statistically significant improvement in disease severity in the treatment groups compared to those of control groups. The three wavelengths used demonstrated efficacy, and a clear dose-response curve was observed for 850 nm. On day 11, colonoscopic scoring in the sham-treated mice increased, while activity in all treated groups remained stable. From these observations, photobiostimulation with LLLT has a significant positive effect on disease progression in mice with dextran sodium sulfate induced-colitis (Zigmond, Varol, Kaplan, Shapira, & Melzer, 2014).

LLLT has been widely used in the field of dermatology, and a study by Avci et al. broadly investigated the use of LLLT in skin pathologies and the underlying mechanisms

in skin rejuvenation. Although skin is naturally exposed to light more than any other organ, it still responds well to red and near-infrared wavelengths. The photons are absorbed by mitochondrial chromophores in skin cells. Consequently, electron transport, release of ATP and NO, blood flow, and ROS all increase, and varying signaling pathways are activated. Stem cells can be activated as well, allowing increased tissue repair and healing. LLLT is also known to have beneficial effects on wrinkles, acne scars, and hypertrophic scars, and it has been used in healing of burns, and reducing UV damage both as a treatment and as a prophylactic measure. In pigmentary disorders such as vitiligo, LLLT can increase pigmentation by stimulating melanocyte proliferation, and reduce depigmentation by inhibiting autoimmunity. Inflammatory diseases such as psoriasis and acne can also be managed through LLLT (Avci, et al., 2013).

Tissue penetration depth of LLL varies on the wavelength as illustrated in Figure 5. LLLT uses light with wavelengths between 390 and 1100 nm and can be continuous wave or pulsed. Wavelengths in the range of 390–600 nm are used to treat superficial tissue, and longer wavelengths in the range of 600–1100 nm, which penetrate further, are used to treat deeper-seated tissues. Wavelengths in the range of 700–750 nm have been found to have limited biochemical activity and are therefore not often used (Avci, et al., 2013). Tissue penetration depth of LLL also varies with energy density. High energy densities are used on superficial tissues, and low energy densities are used on deep tissues. 3 J/cm^2 is the most commonly used dose in clinical scenarios.

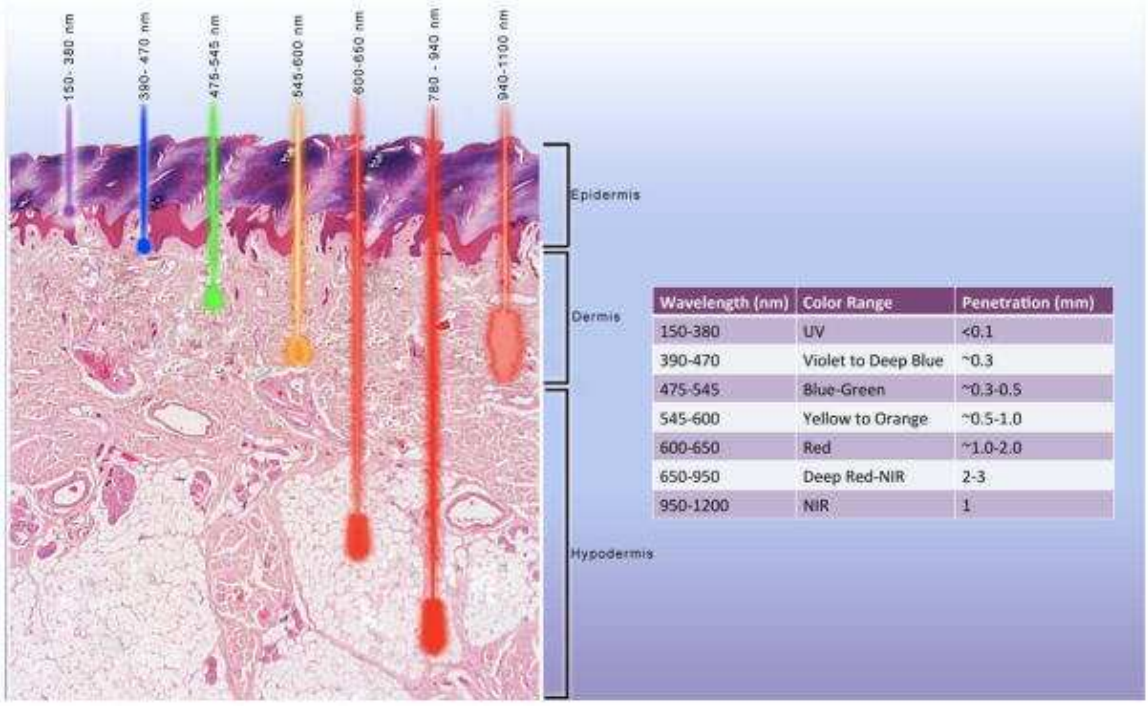

Figure 5. Tissue penetration depths of various wavelengths. Abbreviations: UV: Ultra-Violet, NIR: Near-Infra Red (Avci, et al., 2013).

A number of studies investigated the mechanisms of skin rejuvenation under LLLT. Studies by Abergel et al. and Yu et al. reported an increase in production of pro-collagen, collagen, basic fibroblast growth factor (bFGF) and proliferation of fibroblasts after exposure to low-energy laser irradiation in vitro and in vivo animal models (Abergel, Lyons, Castel, Dwyer, & Uitto, 1987), (Yu, Naim, & Lanzafame, 1994). Furthermore, it was observed that LLLT increased microcirculation and vascular perfusion in the skin, and altered the amount of platelet derived growth factor (PDGF) and transforming growth factor-β1 (TGF-β1), and inhibited apoptosis (Chung, et al., 2012), (Schindl, Heinze, Schindl, Pernerstorfer-Schon, & Schindl, 2002), (Ben-Dov, et al., 1999). A study by Barolet et al. used a 3-dimensional model of tissue-engineered human reconstructed skin

to investigate the potential of 660 nm, 4 J/cm^2 LED in modulating collagen and matrix metalloproteinase-1 (MMP-1), and the results showed upregulation of collagen and downregulation MMP-1 in vitro. An increase in the amount of tissue inhibitor of metalloproteinase (TIMP) may have prevented the proteolytic degradation of collagen by decreasing the amount of MMP-1 (Barolet, Roberge, Auger, Boucher, & Germain, 2009). From the studies mentioned above, it can be concluded that the underlying molecular changes in response to LLLT aid skin rejuvenation through increasing collagen production and decreasing collagen degradation as illustrated in Figure 6.

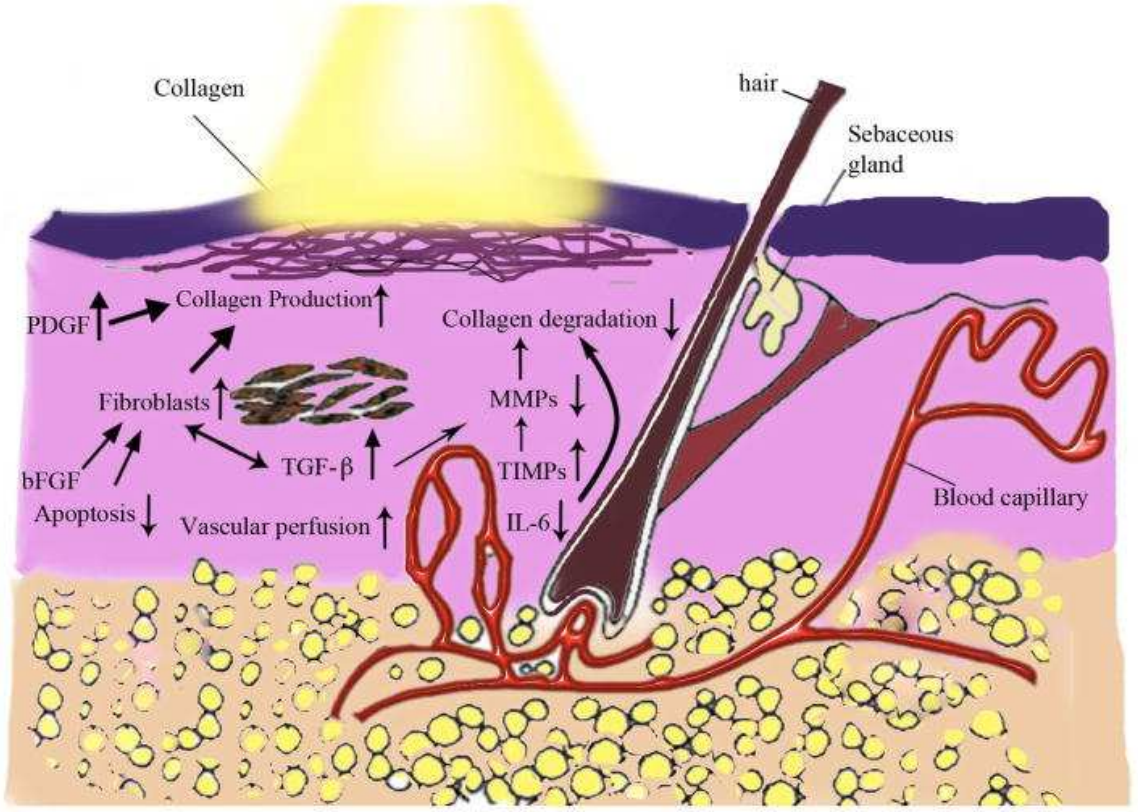

Figure 6. Possible mechanism of actions of skin rejuvenation under LLLT. Abbreviations: bFGF: basic Fibroblast Growth Factor, IL-6: Interleukin-6, LLLT: Low Level Light Therapy, MMP: Matrix Metalloproteinase, PDGF: Platelet-derived Growth Factor, TGF-β: Transforming Growth Factor-β, TIMP: Tissue Inhibitor of Metalloproteinase (Avci, et al., 2013).

The safety, effectiveness, and biochemical mechanisms of LLLT have been broadly studied both in vitro and in vivo, but there has been no clear consensus in the validity of its use, and in choosing the ideal parameters (wavelength, energy density, and duration of exposure etc). In fact, it has been withheld by practitioners with a fear that LLL could potentially cause cell proliferation and promote the growth of cancer. Moreover, there has been little scientific study of oncologic outcomes after use of LLLT in cancer patients. From this standpoint, there is clearly a need for further studies of any potential oncogenesis of LLL in the presence or the absence of a given chemotherapeutic drug.

Specific Aims

To evaluate the safety of LLLT on cancer cells in the presence or the absence of a chemotherapeutic drug, we will

1) Determine the IC_{50} concentrations of two different anti-cancer chemotherapeutic drugs (5-FU and cisplatin) in two human cancer cells (MCF-7 and Jurkat E6-1).
2) Determine the viability of both cells after treating each with LLL (808 nm, varying energy densities) both in the absence and the presence of each anti-cancer chemotherapeutic drug at a final concentration of one IC_{50}.
3) Perform statistical analyses to determine if there is a significant difference in the viability of cells between control (0 J/cm^2) and each energy density (range from 0.1 J/cm^2 to 10 J/cm^2) for both cell lines with each anti-cancer chemotherapeutic drug using three different 1-way ANOVA tests including Bennett, Bonferroni, and Sidak.

We anticipate no significant difference in cell proliferation in both cell lines after LLL application with different energy densities either in the absence or the presence of a specific anti-cancer chemotherapeutic drug. We also don't expect to see any significant difference in the viability of cells between control (0 J/cm^2) and each energy density (range from 0.1 J/cm^2 to 10 J/cm^2) for both cell lines treated with a specific anti-cancer chemotherapeutic drug.

METHODS

Materials

Cell lines

- MCF-7 cell line (American Type Culture Collection (ATCC)), a human breast adenocarcinoma cell line derived from mammary gland.

- Jurkat, Clone E6-1 cell line (ATCC), a human T lymphocytic cell line derived from peripheral blood.

Anti-cancer chemotherapeutic drugs

- 5-FU (Sigma-Aldrich), a potent antitumor agent that inhibits pyrimidine synthesis by inhibiting thymidylate synthetase, thereby, depleting intracellular deoxythymidine triphosphate (dTTP) pools (Sigma-Aldrich).

- Cisplatin (Sigma-Aldrich), a potent platinum-based antitumor agent that forms cytotoxic adducts with the DNA, primarily intrastrand crosslink adducts, which activate several signal transduction pathways, and culminate in the activation of apoptosis (Siddik, 2003).

LLL sources

LED device (Photo therapeutics, Inc.) was used to apply LLL on each cell line with a non-coherent light of 808 nm and power density of 0.014 W/cm^2. The energy density was calculated by the following formula:

Power density (0.014 W/cm^2) x Time (s) = Energy Density (J/cm^2)

The application of each energy density of LLL required the use of different exposure time for each.

Table 1. An example of a range of varying energy densities applied during an actual procedure

Energy Density (J/cm^2)	0	0.1	0.5	1	3	10
Time (seconds)	~ 0	~ 7	~ 36	~ 71	~ 214	~ 714

Cell Counting Kit-8 (CCK-8) solution (Dojindo) used for the detection of viable cells

CCK-8 allows sensitive colorimetric assays for the determination of the number of viable cells in cell proliferation and cytotoxicity assays by utilizing Dojindo's highly water soluble tetrazolium-8 (WST-8) salt. This monosodium salt is reduced by dehydrogenases in cells in the presence of an electron mediator to yield formazan which is an orange colored product that is soluble in culture medium. The amount of the formazan dye generated by dehydrogenases in cells is directly proportional to the number of living cells (Dojindo Molecular Technologies, Inc., 2013).

Flow chart of the experimental procedures

1. Recovery of each cell line

2. Determination of IC_{50} values of 5-FU and cisplatin separately on each cell line

MCF-7 cell line

1) Seeding MCF-7 cells into 96-well plate

⇩ ~ 24-hour incubation

2) Treatment of cells with varying concentrations of 5-FU and cisplatin separately

⇩ ~ 48-hour incubation

3) Treatment of cells with CCK-8 solution

⇩ ~ 2-hour incubation

4) Detection of viable cells

* A total of 3 trials and 4 trials were done for the determination of IC_{50} value of cisplatin and 5-FU, respectively.

Jurkat E6-1 cell line

1) Seeding Jurkat E6-1 cells with varying concentrations of 5-FU and cisplatin separately into 96-well plate

⇩ ~ 48-hour incubation

2) Addition of CCK-8 solution

⇩ ~ 2-hour incubation

3) Detection of viable cells

* A total of 4 trials were done for the IC_{50} determinations of both 5-FU and cisplatin

3. LLLT on each cell line in the presence and the absence of 5-FU and cisplatin using IC_{50} value of each

MCF-7 cell line

1) Seeding MCF-7 cells into 96-well plate

⇩ ~ 24-hour incubation

2) Treatment of cells with and without 5-FU (70 μM) and cisplatin (17 μM) separately followed by the application of LLL with different dose densities

⇩ ~ 48-hour incubation

3) Treatment of cells with CCK-8 solution

⇩ ~ 2-hour incubation

4) Detection of viable cells

* A total of 5 trials were done for both 5-FU and cisplatin treatments

Jurkat E6-1 cell line

1) Seeding Jurkat E6-1 cells with and without 5-FU (20 μM) and cisplatin (7 μM) separately followed by the application of LLL with different dose densities

⇩ ~ 48-hour incubation

2) Addition of CCK-8 solution

⇩ ~ 2-hour incubation

3) Detection of viable cells

* A total of 3 trials were done for both 5-FU and cisplatin treatments

Figure 7. Flow chart of the procedure taken for LLLT on each cell line under the treatment of 5-FU and cisplatin separately. Abbreviations: CCK-8: Cell Counting Kit-8, IC_{50}: the half maximal inhibitory concentration, LLL: Low Level Light, LLLT: Low Level Light Therapy, MCF-7: Michigan Cancer Foundation-7, 5-FU: 5-Fluorouracil.

Notes

- All solutions and equipments used were sterile, and the procedures were performed using aseptic techniques to prevent contamination.

- All culture incubations were performed in a humidified 37°C, 5% CO_2 incubator.

- When using CCK-8 solution, light was turned off since CCK-8 solution is light sensitive.

- To keep MCF-7 cells mitogenic, 4 mg/ml insulin solution (Novolin) was added to MCF-7 cell solution. For a 5 ml MCF-7 solution, 12 µl of insulin solution was added.

- To make full medium, Roswell Park Memorial Institute-1640 (RPMI-1640) base medium (Lonza), Fetal Bovine Serum (Atlanta Biologicals), 0.5M Penicillin/Streptomycin solution (Gibco), and 100% 200 mM L-glutamine solution (Gibco) were mixed in 88%, 10%, 1%, and 1% in volume proportion respectively.

- 1 mM 5-FU stock solution, 1.7 mM cisplatin stock solution, and insulin solution were vortexed before being used.

- For MCF-7 cells, cells that were small and round whether attached or detached were considered dead.

Detailed procedures

Recovery of MCF-7 cell line

1. A screw-cap vial containing MCF-7 cell line was collected from liquid nitrogen storage, and placed in a 37°C water bath along with 10 ml of serum-free medium.

2. The frozen cells were allowed to thaw inside the water bath for 2–3 minutes with constant agitation to quickly thaw the cells.

3. 1 ml of thawed cells was transferred to 10 ml of serum-free medium, and mixed thoroughly.

4. The mixture was centrifuged at 900 rpm for 5 minutes, and the supernatant was discarded.

5. 5 ml of full medium was added to the cells (pellet), and mixed thoroughly. Then, the cell suspension was transferred into a culture flask.

6. 12 µl of insulin solution was added to the cell suspension, and the cell suspension was visualized to confirm the viability of the cells. Then, the flask was placed inside the incubator.

Subculture of MCF-7 cell line and medium renewal

MCF-7 cell line was sub-cultured once confluent (above 80% coverage), and medium was renewed 2 or 3 times a week.

1. The full medium was discarded, and the cell monolayer was washed with 5 ml of phosphate-buffered saline (PBS) solution (Lonza).

2. 500 µl of 0.25% trypsin solution (Gibco) was added to wash cell monolayer making sure the solution covers the entire monolayer. Then, the solution was discarded.

3. The cells were incubated for 1–2 minutes or additional minutes (not exceeding 5 minutes) to make sure the cells are detached.

4. The cells were resuspended with 5 ml full medium, and transferred into a new flask with new full medium in either 1:3 or 1:4 ratio depending on the confluence.

5. 12 µl of insulin solution was added to the flask, and the cell suspension was visualized to confirm the viability of the cells. Then, the flask was placed inside the incubator.

Seeding MCF-7 cells into 96-well plate

1. The cells were washed and detached by following the procedure described in the section “Subculture of MCF-7 cell line and medium renewal” from 1 to 3.

2. 5 ml of full medium was placed into the flask, and mixed thoroughly.

3. 15 µl of 0.4% trypan blue solution (Gibco) and 15 µl of MCF-7 cell solution were combined, and they were mixed thoroughly. Then, 15 µl of the mixture was placed into a counting slide (Biorad).

4. The number of cells was counted with a tissue culture (TC) 10^{TM} automated cell counter (Biorad).

5. Based on the number of cells, the amounts of cell suspension, full medium, and insulin solution needed were calculated such that 100 µl containing approximately 5000 cells are placed into each well.

6. The calculated amounts of cell suspension, full medium, and insulin solution were combined, and mixed thoroughly.

7. 100 µl (~5000 cells) of mixture was placed into each well in triplicate or quintuplicate per column.

8. The cells were incubated for approximately 24 hours.

Treatment of MCF-7 cells with varying concentrations of 5-FU and cisplatin separately

1. Varying concentrations of 5-FU or cisplatin solutions were made by combining calculated amounts of 5-FU or cisplatin stock solution, full medium, and 1.44 µl of insulin solution (quintuplicate) or 0.96 µl of insulin solution (triplicate) for each concentration. Then, the mixtures were vortexed.

2. The full medium was drawn out from each well using a vacuum.

3. Each column was treated with 100 µl of each different concentration of 5-FU or cisplatin solution

4. The 96-well plate was placed inside the incubator for approximately 48 hours.

Treatment of MCF-7 cells with CCK-8 solution

1. The amounts of full medium and CCK-8 solution needed were calculated based on the fact that 100 µl of full medium and 10 µl of CCK-8 solution were needed for each well.

2. The calculated amounts of full medium and CCK-8 solution were combined, and mixed thoroughly.

3. Full medium was drawn out from each well using a vacuum.

4. 110 µl of the mixture was dispensed into each well making sure that bubbles are not formed. If the bubbles were formed, they were eliminated by gently tipping it with 10 µl pipette tip.

5. The 96-well plate was placed inside the incubator for approximately two hours.

Detection of viable cells

1. The 96-well plate was inserted into a microplate reader (Molecular Devices), and the absorbance values were measured at 450 nm using Softmax Pro 6.4 (Molecular Devices).

Treatment of MCF-7 cells with and without 5-FU (70 µM) and cisplatin (17 µM) separately followed by application of LLL using different dose densities

1. The calculated amounts of full medium and insulin solution were combined, and mixed thoroughly. The calculated amounts of full medium, 5-FU stock solution or cisplatin stock solution, and insulin solution were combined, and mixed thoroughly.

2. Full medium was drawn out from each well using a vacuum.

3. Cells on one half (first 6 columns) of the 96-well plate were not treated with 5-FU or cisplatin. Each well was treated with 100 µl of mixture containing full medium and insulin solution. Cells on the other half (last 6 columns) were treated with 70 µM solution

of 5-FU or 17 μM solution of cisplatin. On this half, 100 μl of the mixture containing full medium, 5-FU stock solution or cisplatin stock solution, and insulin solution was placed into each well.

4. The 96-well plate was covered with its lid, and aluminum foil was wrapped around the lid while exposing each column one at a time from left to right when applying LLL. Each column was treated with LLL by an LED device for different duration of time, thus varying dose densities ranging from 0 to 10 J/cm^2 were applied to each column. The same set of dose densities were applied for both halves.

5. The 96-well plate was placed inside the incubator for approximately 48 hours.

Recovery of Jurkat E6-1 cell line

The same procedure was taken as the section "Recovery of MCF-7 cell line" except insulin solution was not added to the cell suspension.

Subculture of Jurkat E6-1 cell line and medium renewal

The cells were passaged about twice a week to maintain the cell density at a concentration between 1 x 10^5 cells/ml and 1 x 10^6 cells/ml, making sure that the concentration does not exceed 3 x 10^6 cells/ml. Medium was renewed every 2–3 days depending on cell density.

1. 100 μl cell suspension and 300 μl of full medium were combined, and mixed thoroughly.

2. 10 μl of the mixture was mixed thoroughly with 10 μl trypan blue solution.

3. 10 μl of the mixture from above was transferred to edge of hemocytometer counting chamber (Haussen Scientific), and a cover slip was placed on top of the mixture.

4. The counting chamber was viewed under the microscope, and out of 9 squares, the central square was positioned to the center, and viewed with 10x power. The number of cells in the four corners (four squares) was counted. For the cells that were positioned in the lines of each square, only the ones that were positioned in the top and the left side of each square were counted.

* Cells that appeared blue were considered dead, and they were not counted.

5. The cell density was calculated as below.

Cells/ml = Average count per square x dilution factor x 10^4 = Total # of cells in the four corners/4 x 8 x 10^4

6. The cell suspension was centrifuged at 1000 rpm for 5 minutes.

7. The supernatant was discarded, and 5 ml full medium was added to suspend the cells.

8. The split ratio of cell suspension and full medium was determined based on the cell density, and the amounts needed for the cell suspension and full medium were determined.

9. The calculated amounts of mentioned above were combined into a new flask before incubation.

<u>Seeding Jurkat E6-1 cells with varying concentrations of 5-FU and cisplatin separately into 96-well plate</u>

1. The cell density was determined following the procedure described in the section "Subculture of Jurkat E6-1 cell line and medium renewal" from step 1 to 5.

2. For each concentration of 5-FU or cisplatin solution, the amounts needed for cell suspension, 5-FU or cisplatin stock solution, and full medium were calculated based on the cell density and the concentration of the solution to be made.

3. The calculated amounts mentioned above were combined, and the combined mixtures were vortexed.

4. Each column was treated with 100 µl of each mixture in quintuplicate.

5. The 96-well plate was placed inside the incubator for approximately 48 hours.

Addition of CCK-8 solution into Jurkat E6-1 cells

1. 10 µl of CCK-8 solution was dispensed into each well. If bubbles were formed, they were eliminated by gently tipping it with 10 µl pipette tip.

2. The 96-well plate was placed inside the incubator for approximately two hours.

Seeding Jurkat E6-1 cells with and without 5-FU (20 µM) and cisplatin (7 µM) separately followed by application of LLL using different dose densities

1. The cell density of the cell suspension was determined following the procedure described in section "Subculture of Jurkat E6-1 cell line and medium renewal" from step 1 to 5.

2. Based on the cell density, the amounts needed for cell suspension and full medium were calculated for the wells that were not going to be treated with 5-FU or cisplatin. Also, the amounts of cell suspension, full medium, 5-FU stock solution or cisplatin stock solution were calculated for the wells that were going to be treated with 20 µM solution of 5-FU or 7 µM solution of cisplatin.

3. The calculated amounts mentioned above were combined, and mixed thoroughly for each.

4. Cells on one half (the first 6 columns) of the 96-well plate were not treated with 5-FU or cisplatin. Each well on this half was treated with 100 µl of the mixture containing cell suspension and full medium. Cells on the other half (the next 6 columns) were treated with 20 µM solution of 5-FU or 7 µM solution of cisplatin. On this half, 100 µl of the mixture containing cell suspension, full medium, and 5-FU stock solution or cisplatin stock solution was placed into each well.

5. Step 4 to 5 in section "Treatment of MCF-7 cells with and without 5-FU (70 µM) and cisplatin (17 µM) separately followed by application of LLL using different dose densities" was repeated.

RESULTS

Determination of IC_{50} values of 5-FU and cisplatin on MCF-7 and Jurkat E6-1 cell lines

To determine the IC_{50} of each drug, each cell line was treated with different concentrations of each drug for 48 hours, and then the cell viability was measured. IC_{50} was determined as the concentration of each drug required for 50% inhibition of the cell viability.

Multiple trials were done as depicted in Figure 7 to determine the IC_{50} values of 5-FU and cisplatin on each cell line. The range of concentration was varied, and the number of concentrations used was varied throughout the trials depending on the outcomes for each trial. From each trial, simple linear regression was performed, and the IC_{50} value was determined from the regression line. Out of multiple IC_{50} values determined, the value that had the best fit along the points with a high R^2 value was chosen. The IC_{50} values of 5-FU and cisplatin on MCF-7 and Jurkat E6-1 cell lines were determined as Table 2.

Table 2. IC_{50} values of 5-FU and cisplatin on MCF-7 and Jurkat E6-1 cell lines

Cell lines / Anti-cancer chemotherapeutic drugs	MCF-7	Jurkat E6-1
5-FU	70 μM	20 μM
Cisplatin	17 μM	7 μM

Abbreviations: IC_{50}: the half maximal inhibitory concentration, MCF-7: Michigan Cancer Foundation-7, 5-FU: 5-Fluorouracil.

The four graphs in the Figure 8 show the simple linear regression lines for each anti-cancer chemotherapeutic drug on each cell line. Each simple linear regression line represents the line that displayed the best fit along the points out of multiple simple linear regression lines obtained from all trials for each anti-cancer chemotherapeutic drug on each cell line.

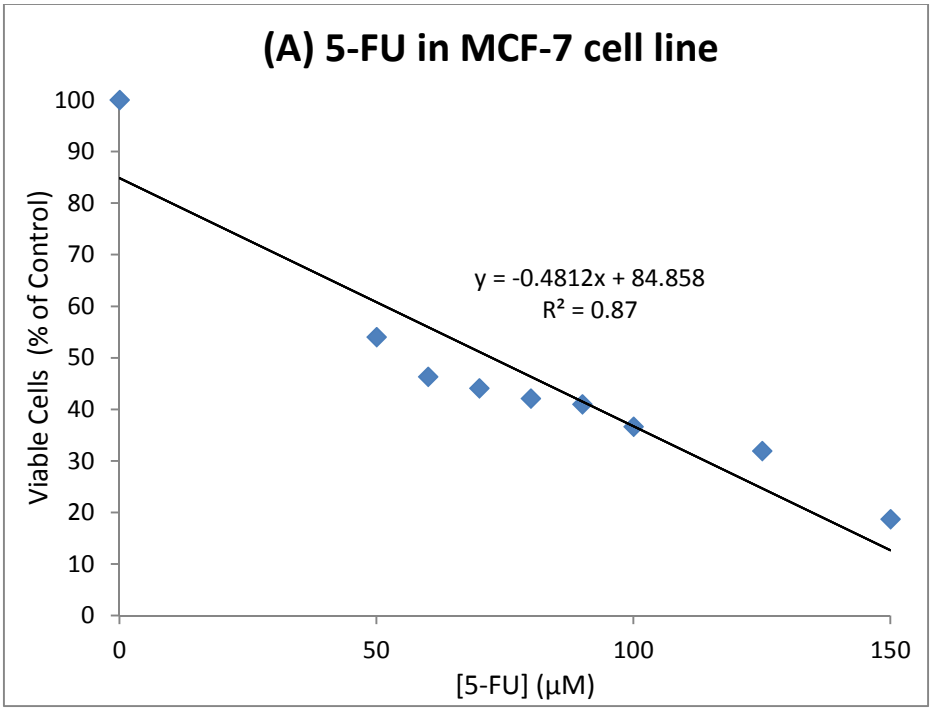

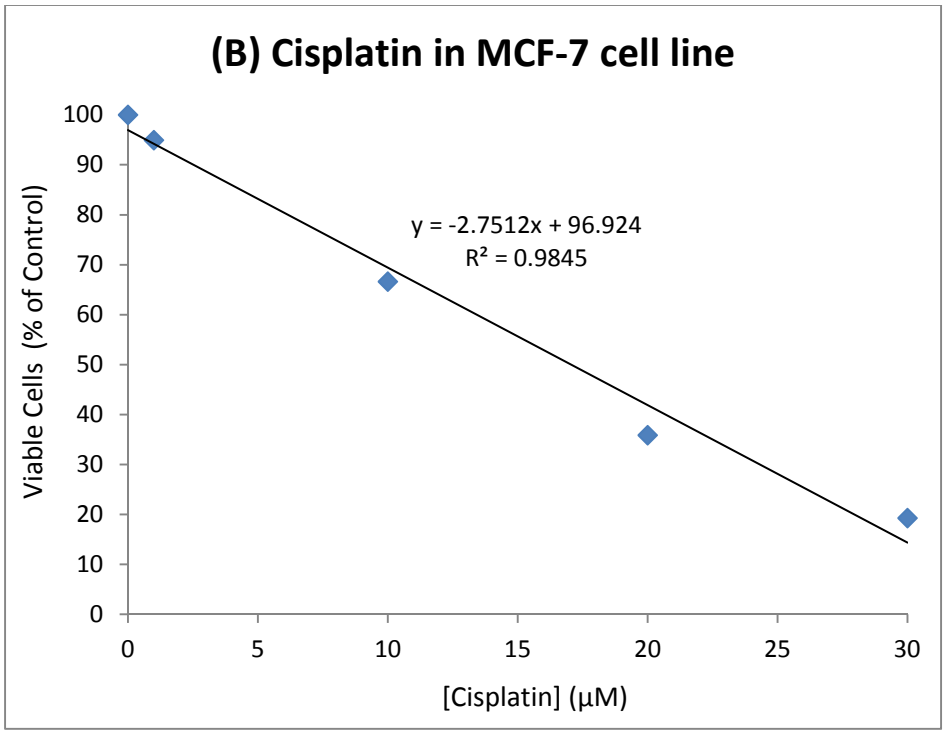
(B) Cisplatin in MCF-7 cell line
Viable Cells (% of Control)
100
90
80
70
60
50
40
30
20
10
0
y = -2.7512x + 96.924
R² = 0.9845
0
5
10
15
20
25
30
[Cisplatin] (µM)

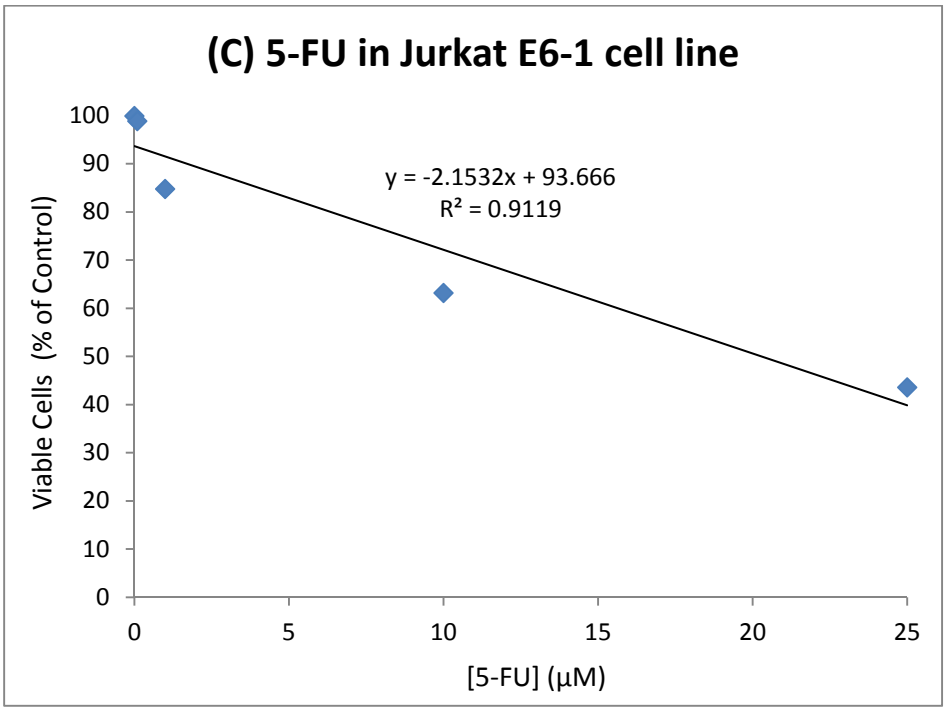
(C) 5-FU in Jurkat E6-1 cell line
Viable Cells (% of Control)
100
90
80
70
60
50
40
30
20
10
0
y = -2.1532x + 93.666
R² = 0.9119
0
5
10
15
20
25
[5-FU] (µM)

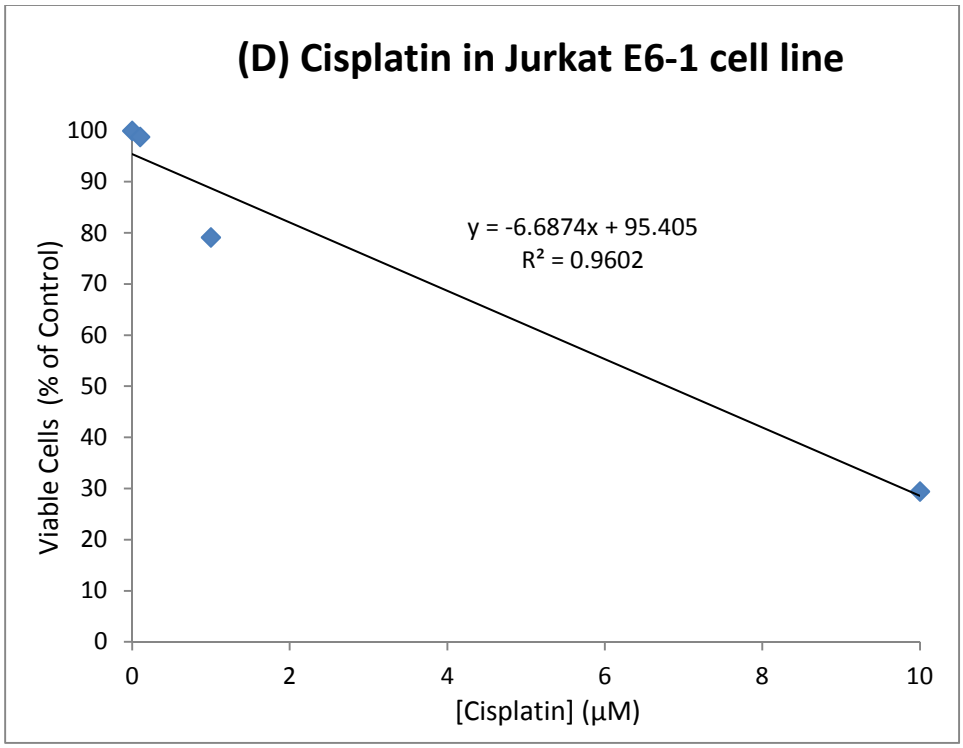

Figure 8. Simple linear regression lines for the determination of IC_{50} values of 5-FU and cisplatin in MCF-7 and Jurkat E6-1 cell lines. (A) 5-FU in MCF-7 cell line, [5-FU] (μM) = [0, 50, 60, 70, 80, 90, 100, 125, 150] (μM) (B) Cisplatin in MCF-7 cell line, [cisplatin] (μM) = [0, 1, 10, 20, 30] (μM) (C) 5-FU in Jurkat E6-1 cell line, [5-FU] (μM) = [0, 0.1, 1, 10, 25] (μM) (D) Cisplatin in Jurkat E6-1 cell line, [cisplatin] (μM) = [0, 0.1, 1, 10] (μM). Abbreviations: IC_{50}: the half maximal inhibitory concentration, MCF-7: Michigan Cancer Foundation-7, 5-FU: 5-Fluorouracil.

Application of LLL on MCF-7 and Jurkat E6-1 cell lines under the treatment of 5-FU and cisplatin

To determine the effect of LLL on the viability of both cell lines, cell viability of drug-treated and non-treated group was measured after applying LLL with different energy densities. The viability of cells that were treated with different energy densities of LLL was compared to that of control (0 J/cm^2). The statistic analysis was performed by GraphPad software, and three different types of 1-way ANOVA multiple comparisons tests including Bennett, Bonferroni, and Sidak were done for each comparison. For each

group, the mean value of each energy density was compared with the mean value of the control (0 J/cm^2). The results of significance tests in the viability of cells between different energy densities and the control (0 J/cm^2) for both groups for each anti-cancer chemotherapeutic drug on each cell line are indicated in Tables 3–6. Also graphs were made as in the Figure 9 showing the number of viable cells (% to control) for each energy density of LLL for both the non-treated group and the drug-treated group for each cell line.

Significance in the number of viable cells for each energy density compared to the control (0 J/cm^2) of each group

When LLL was applied on MCF-7 cells, there was no significant difference in the number of viable cells between each energy density and the control (0 J/cm^2) in the absence or the presence of 5-FU at IC_{50} (70 μM). However, a slight increasing trend among the number of viable cells was observed with increasing energy density in the absence of 5-FU, whereas no specific trend among the number of viable cells was observed with increasing energy density in the presence of 5-FU at IC_{50} (70 μM).

There was no significant difference in the number of viable cells between each energy density and the control (0 J/cm^2) in the absence or the presence of cisplatin at IC_{50} (17 μM). No specific trend among the number of viable cells was observed with increasing energy density in the absence or the presence of cisplatin at IC_{50} (17 μM).

When LLL was applied on Jurkat E6-1 cells, there was no significant difference in the number of viable cells between each energy density and the control (0 J/cm^2) in the absence or the presence of 5-FU at IC_{50} (20 μM). No specific trend in the number of

viable cells was observed with increasing energy density in the absence or the presence of 5-FU at IC_{50} (20 μM).

There was no significant difference in the number of viable cells between each energy density and the control in the absence of cisplatin. However, a significant increase ($0.01 < P < 0.05$) in the number of viable cells was confirmed between control group (0 J/cm^2) and 10 J/cm^2 of LLL-treated group in the presence of cisplatin at IC_{50} (7 μM). All three tests including Bennett, Bonferonni, and Sidak tests confirmed its significance. No significant difference in the number of viable cells was found among the remaining comparisons for the cisplatin-treated group. No specific trend in the number of viable cells was observed with increasing energy density in the absence or the presence of cisplatin at IC_{50} (7 μM).

Table 3. Significance tests results for LLLT on MCF-7 cell line in the absence and the presence of 5-FU

Groups and Comparisons (J/cm^2) / Tests	Non-treatment group (without 5-FU)					Treatment group (with 5-FU at 70 μM)				
	0 vs. 0.1	0 vs. 0.5	0 vs. 1	0 vs. 3	0 vs. 10	0 vs. 0.1	0 vs. 0.5	0 vs. 1	0 vs. 3	0 vs. 10
Bennett	NS	NS	NS	NS	NS	NS	NS	NS	NS	NS
Bonferroni	NS	NS	NS	NS	NS	NS	NS	NS	NS	NS
Sidak	NS	NS	NS	NS	NS	NS	NS	NS	NS	NS

Abbreviations: LLLT: Low Level Light Therapy, MCF-7: Michigan Cancer Foundation-7, NS: No Significance ($P > 0.05$), 5-FU: 5-Fluorouracil.

Table 4. Significance tests results for LLLT on MCF-7 cell line in the absence and the presence of cisplatin

Groups and Comparisons (J/cm^2) / Tests	Non-treatment group (without cisplatin)					Treatment group (with cisplatin at 17 μM)				
	0 vs. 0.1	0 vs. 0.5	0 vs. 1	0 vs. 3	0 vs. 10	0 vs. 0.1	0 vs. 0.5	0 vs. 1	0 vs. 3	0 vs. 10
Bennett	NS	NS	NS	NS	NS	NS	NS	NS	NS	NS
Bonferroni	NS	NS	NS	NS	NS	NS	NS	NS	NS	NS
Sidak	NS	NS	NS	NS	NS	NS	NS	NS	NS	NS

Abbreviations: LLLT: Low Level Light Therapy, MCF-7: Michigan Cancer Foundation-7, NS: No Significance ($P > 0.05$).

Table 5. Significance tests results for LLLT on Jurkat E6-1 cell line in the absence and the presence of 5-FU

Groups and Comparisons (J/cm^2) / Tests	Non-treatment group (without 5-FU)					Treatment group (with 5-FU at 20 μM)				
	0 vs. 0.1	0 vs. 0.5	0 vs. 1	0 vs. 3	0 vs. 10	0 vs. 0.1	0 vs. 0.5	0 vs. 1	0 vs. 3	0 vs. 10
Bennett	NS	NS	NS	NS	NS	NS	NS	NS	NS	NS
Bonferroni	NS	NS	NS	NS	NS	NS	NS	NS	NS	NS
Sidak	NS	NS	NS	NS	NS	NS	NS	NS	NS	NS

Abbreviations: LLLT: Low Level Light Therapy, NS: No Significance ($P > 0.05$), 5-FU: 5-Fluorouracil.

Table 6. Significance tests results for LLLT on Jurkat E6-1 cell line in the absence and the presence of cisplatin

Groups and Comparisons (J/cm^2) / Tests	Non-treatment group (without cisplatin)					Treatment group (with cisplatin at 7 μM)				
	0 vs. 0.1	0 vs. 0.5	0 vs. 1	0 vs. 3	0 vs. 10	0 vs. 0.1	0 vs. 0.5	0 vs. 1	0 vs. 3	0 vs. 10
Bennett	NS	NS	NS	NS	NS	NS	NS	NS	NS	*
Bonferroni	NS	NS	NS	NS	NS	NS	NS	NS	NS	*
Sidak	NS	NS	NS	NS	NS	NS	NS	NS	NS	*

*: Significance ($0.01 < P < 0.05$). Abbreviations: LLLT: Low Level Light Therapy, NS: No Significance ($P > 0.05$).

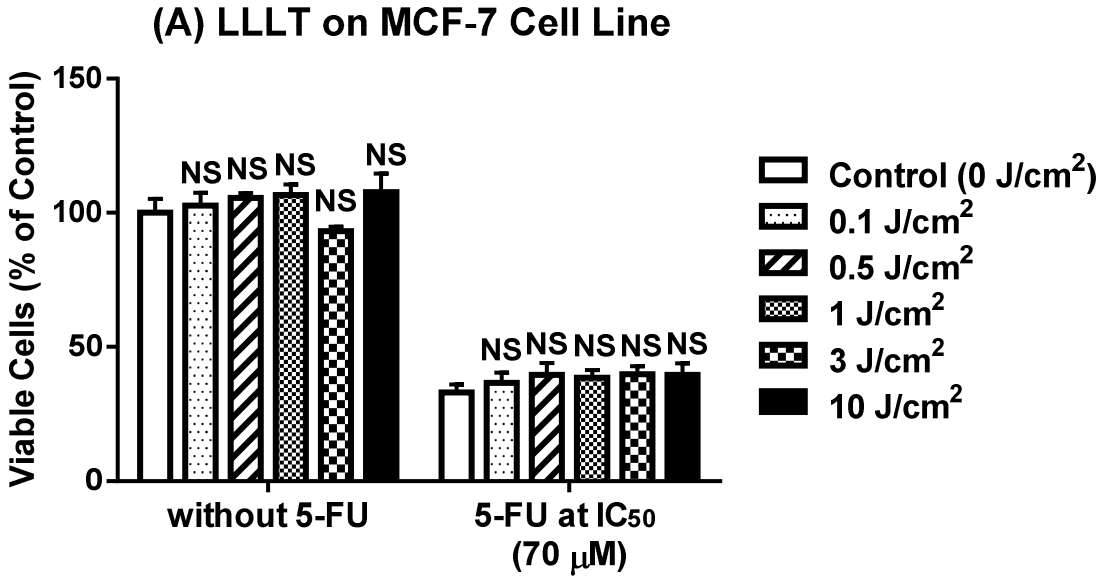
(A) LLLT on MCF-7 Cell Line
Viable Cells (% of Control)
150
100
50
0
NS NS NS NS NS
NS NS NS NS NS
without 5-FU
5-FU at IC50
(70 μM)
Control (0 J/cm2)
0.1 J/cm2
0.5 J/cm2
1 J/cm2
3 J/cm2
10 J/cm2

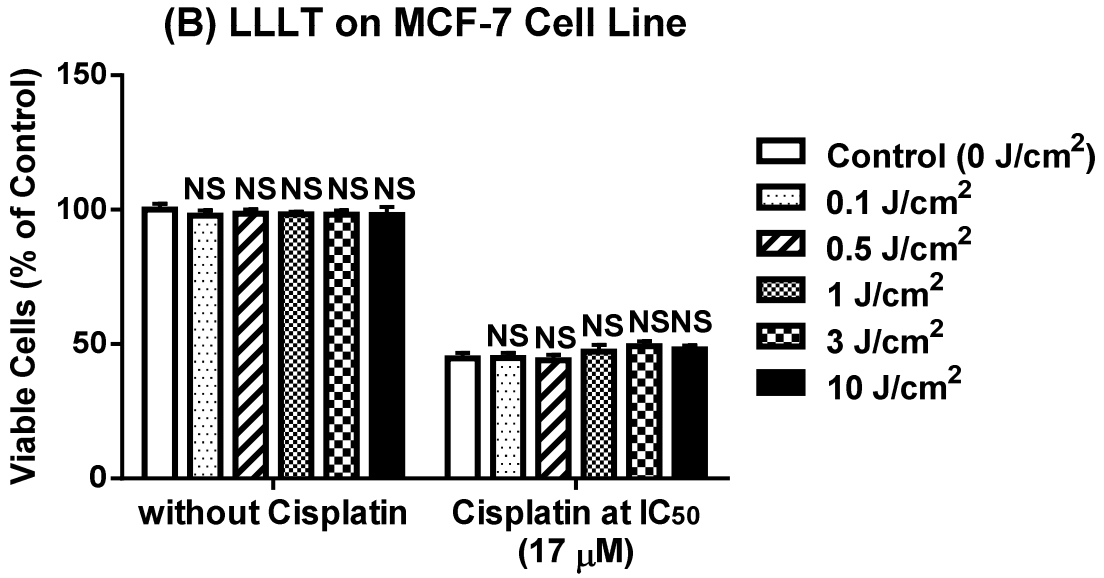
(B) LLLT on MCF-7 Cell Line
Viable Cells (% of Control)
150
100
50
0
NS NS NS NS NS
NS NS NS NSNS
without Cisplatin
Cisplatin at IC50
(17 μM)
Control (0 J/cm2)
0.1 J/cm2
0.5 J/cm2
1 J/cm2
3 J/cm2
10 J/cm2

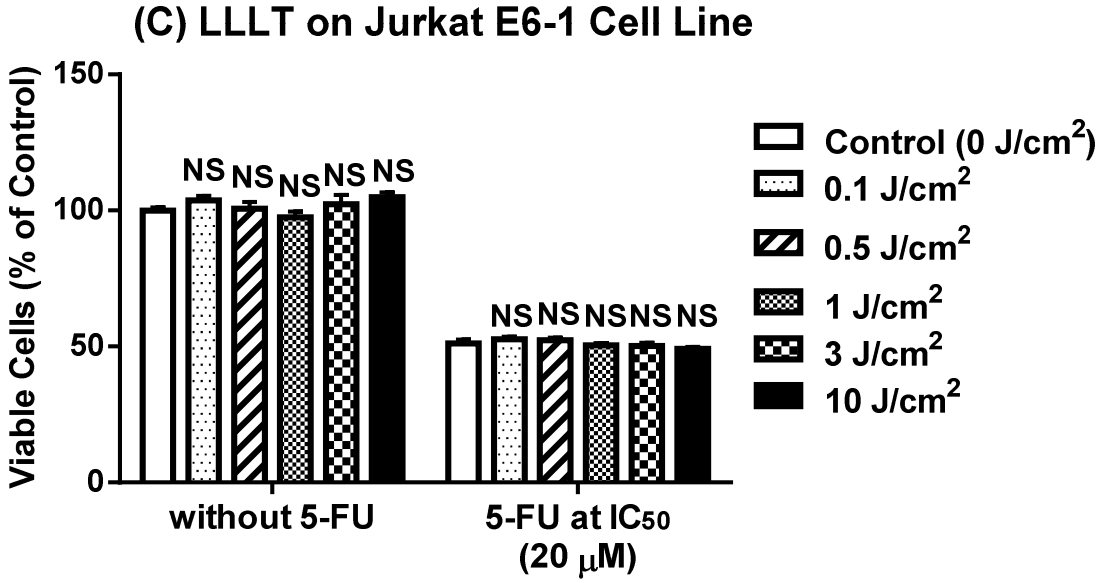

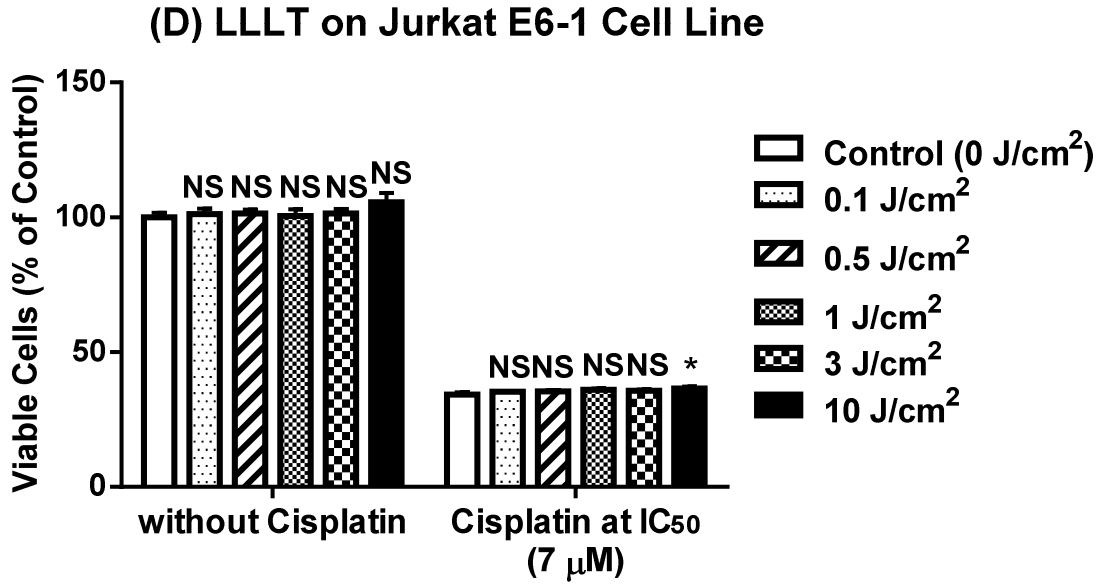

Figure 9. Viability of cells after LLLT with varying energy densities in the absence and the presence of 5-FU or cisplatin. The interleaved bars represent mean values with its standard error of mean. (A) LLLT on MCF-7 cells without and with 5-FU at IC_{50} (70 μM) (B) LLLT on MCF-7 cells without and with cisplatin at IC_{50} (17 μM) (C) LLLT on Jurkat E6-1 cells without and with 5-FU at IC_{50} (20 μM) (D) LLLT on Jurkat E6-1 cells without and with cisplatin at IC_{50} (7 μM). NS: Not significant ($P > 0.05$) compared to the control

(0 J/cm^2), *: Significant (0.01 < P < 0.05) compared to the control (0 J/cm^2). Abbreviations: IC_{50}: the half maximal inhibitory concentration, LLLT: Low Level Light Therapy, MCF-7: Michigan Cancer Foundation-7, NS: No Significance, 5-FU: 5-Fluorouracil.

DISCUSSIONS

Interpretation of results

The treatment of LLL at 808 nm with varying energy densities ranging from 0 J/cm^2 to 10 J/cm^2 under an LED source on MCF-7 and Jurkat E6-1 cells did not induce cell proliferation in vitro either in the absence or the presence of 5-FU or cisplatin at one IC_{50}. Only a single significant difference was observed out of all comparisons as indicated in Tables 3–6. Even the comparison with a significance difference, the difference is imperceptible when looking at the cell viabilities of both groups (control and 10 J/cm^2) in the cisplatin-treated group of Jurkat E6-1 cell line indicated in Figure 9. No definite increase or decrease in trend in the viability of cells was observed with increasing energy density of LLL for all. Although a slight increase in trend in the viability of cells was observed with increasing energy density of LLL when treating LLL on MCF-7 cell in the absence of 5-FU, the trend was not definite. The number of viable cells progressively increased from 0 J/cm^2 to 1 J/cm^2, however, the number of viable cells decreased from 1 J/cm^2 to 3 J/cm^2. In fact, the number of viable cells for 3 J/cm^2 was lower than the number of viable cells for control (0 J/cm^2). The number of viable cells increased from 3 J/cm^2 to 10 J/cm^2. In essence, the number of viable cells was not progressively increasing with each successive increase in energy density, and no definite trend can be concluded from this observation.

Application to cancer patients

The treatment of anti-cancer chemotherapeutic drugs (5-FU and cisplatin) on cancer cell lines (MCF-7 and Jurkat E6-1) could be applicable to clinical situation where chemotherapeutic drugs are treated on cancer patients. LLLT has been used in cancer patients for the treatment of wound healing, relief of pain and inflammation, and other conditions while on chemotherapy. In vitro studies have to be done continuously treating different sources of LLL on different cancer cell lines. Different wavelengths, energy densities, and dosages etc should be tested with different cell lines. The study could be expanded to in vivo studies using animal models.

MCF-7 cell line vs. Jurkat E6-1 cell line

When analyzing results, the results of Jurkat E6-1 cell line were more consistent than those of MCF-7 cell line. Multiple trials of LLLT on each cell line with each drug were done using different energy densities on each trial. Figure 9 shows the results of only one trial for each cell line with each drug. When treating LLL on MCF-7 cells in the absence or the presence of 5-FU or cisplatin, 5 different trials were done for both drugs, and the energy densities applied for each trial were as following: [0, 0.1, 0.5, 1, 3, 10] J/cm^2, [0, 0.1, 1, 2, 5, 10] J/cm^2, [0, 0.5, 1, 2.5, 5, 10] J/cm^2, [0, 0.5, 1, 2, 4, 8] J/cm^2, and [0, 2, 4, 6, 8, 10] J/cm^2. When treating LLL on Jurkat E6-1 cells in the absence or the presence of 5-FU or cisplatin, 3 different trials were done for both drugs, and the energy densities applied for each trial were as following: [0, 0.1, 0.5, 1, 3, 10] J/cm^2, [0, 0.5, 1, 2.5, 5, 10] J/cm^2, and [0, 0.5, 1, 2, 4, 8] J/cm^2. After performing 1-way ANOVA significance tests and observing the trend of cell viability for all the trials for each cell

line with each drug, the one that matched the most with the majority of the results was chosen. For all 4 cases, the trial that applied energy densities [0, 0.1, 0.5, 1, 3, 10] J/cm^2 were chosen, and this happened out of coincidence. For each case, the trial that applied [0, 0.1, 0.5, 1, 3, 10] J/cm^2 was the one that matched the closest to the majority of the results for each. The results of Jurkat E6-1 cell line were precise, however, the results of MCF-7 cell line were not as precise as those of Jurkat E6-1 cell line. In fact, some results were far off from each other with large margin of error. This difference in the preciseness could be due to the difference in the growth property of each cell line. MCF-7 cells are adherent cells in which the cells adhere to the surface of the medium where it grows. When MCF-7 cells were seeded on 96-well plate, and allowed to incubate for 24 hours, the cells adhered to the bottom surface of the well, and stayed attached to it. Jurkat E6-1 cells grow as a single cell suspension with occasional clumping when it's cultured. By being able to float around freely as a single cell, the cells may have been exposed more to the drugs and LLL compare to adherent cells, and this could have been a determining factor for giving consistent results.

Potential sources of error

When counting MCF-7 cells, the cell counter indicated the total number of cells (# of cells/ml) and the total number of live cells (# of cells/ml). The total number of live cells should have been used for calculations, but quite often, the machine indicated much lower total number of live cells compared to the total number of cells even though the cells appeared to be alive. Sometimes, the machine indicated 10–20% yield with the total number of live cells only being 10–20% of the total number of cells. This error may have

been caused by inaccurate differentiation between the live cells and the dead cells by the machine. For these cases, the total number of cells was used for calculations. When seeding MCF-7 cells into 96-well plate, approximately 5000 cells/100 µl of cell suspension had to be used, and calculations were done based on this ratio. However, the total number of live cells may have been over-estimated since the total number of cells was used for some calculations, which may have led to seeding inaccurate number of cells. Out of the all the cells read by the machine, not all cells should have been alive, and by using the total number of cells instead of the total number of live cells, dead cells should have been counted, and this may have contributed to over-estimation. The inaccurate measurement counting the total number of live cells may have been over-ridden by the fact that the total number of viable cells was counted in a relative scale within each well when the viable cells were "read" by the microplate reader to yield absorbance values. However, since there could have been more or fewer than 5000 cells/100 µl within a single well, this may have contributed to inaccurate absorbance values.

When applying LLL on cells, LLL was being emitted from a rectangular area of LED device, and this area was faced down directly into the lid of the 96-well plate into the area of wells of column where LLL was being applied on. During this procedure, there is a possibility that the rectangular area was not properly positioned into the column, and some wells may have not been treated with LLL due to this improper positioning. If this was the case, the cells in the wells that were not applied with LLL would have been the same condition as the cells in control (0 J/cm^2). The possibility of this error is very

low, but there was no guarantee that the rectangular area of the LED device was properly positioned every single time when LLL was applied.

Conclusions

The application of LLL at 808 nm with energy densities ranging from 0.1 J/cm^2 to 10 J/cm^2 under an LED source did not promote cell proliferation or death compared to control (0 J/cm^2) for each cell line in the absence or the presence of each drug, and no definite trend was observed with increasing energy density. The study suggests that LLLT at these parameters may be safe to use on cancer patients, but further studies on different cancer cell lines and animal models are warranted. Moreover, the parameters (wavelength, energy density, dosage) of LLL must be tested further with different cancer lines and animal models.

APPENDIX 1

Raw Data of Figure 8

(A) 5-FU in MCF-7 cell line

[5-FU] (μM)	0	50	60	70	80	90	100	125	150
Absorbance Values	2.2833	1.2177	1.1346	1.0458	0.7521	0.8148	0.5927	0.8272	0.5151
	0.1587	0.9573	1.1249	1.112	1.0274	0.932	0.8458	0.7456	0.4748
	2.5204	1.3452	1.1142	1.0866	0.9356	1.0452	0.8842	0.5907	0.3682
	2.3277	1.3732	1.1072	1.0481	0.9316	0.9795	0.9135	0.6052	0.4884
	2.4614	1.243	1.0708	0.9935	1.1465	0.9758	0.8738	0.725	0.3991
Average Absorbance Values	2.3982	1.294775	1.11034	1.0572	1.010275	0.983125	0.879325	0.765933	0.44912
% of control (0 μM)	100	53.98945	46.29889	44.08306	42.12639	40.99429	36.66604	31.93784	18.72738

(B) Cisplatin in MCF-7 cell line

[Cisplatin] (μM)	0	1	10	20	30
Absorbance Values	2.4671	2.2412	1.5915	0.7507	0.54
	2.4476	1.9188	1.9291	0.7938	0.5771
	2.5314	2.2297	1.5317	0.9581	0.5151
	2.2512	2.348	1.7405	0.8398	0.3397
	2.4689	2.426	1.6208	1.024	0.376
Average Absorbance Values	2.43324	2.311225	1.621125	0.87328	0.46958
% of control (0 μM)	100	94.98549	66.624131	35.8895958	19.298548

(C) 5-FU in Jurkat E6-1 cell line

[5-FU] (μM)	0	0.1	1	10	25
Absorbance Values	0.5271	0.5505	0.4498	0.3844	0.2365
	0.5841	0.567	0.4363	0.3614	0.227
	0.5488	0.4966	0.0899	0.3156	0.2746
	0.5397	0.5314	0.4016	0.3114	0.2179
	0.5129	0.5372	0.5533	0.3421	0.228
Average Absorbance Values	0.54252	0.53654	0.46025	0.34298	0.2368
% of control (0 μM)	100	98.89774	84.83558	63.21979	43.64816

(D) Cisplatin in Jurkat E6-1 cell line

[Cisplatin] (μM)	0	0.1	1	10
Absorbance Values	0.4514	0.4721	0.332	0.1315
	0.4715	0.4461	0.3553	0.1309
	0.4812	0.4392	0.3548	0.1399
	0.442	0.4601	0.4001	0.1328
	0.4335	0.4347	0.362	0.1362
Average Absorbance Values	0.45592	0.45044	0.36084	0.13426
% of control (0 μM)	100	98.79803	79.14546	29.44815

APPENDIX 2

Raw Data of Figure 9

(A) LLLT on MCF-7 cells without and with 5-FU at IC_{50} (70 μM)

	without 5-FU							with 5-FU (70 uM)					
Energy Density (J/cm^2)	0	0.1	0.5	1	3	10		0	0.1	0.5	1	3	10
Absorbance Values	1.7512	1.2703	1.5721	1.5449	1.4264	1.4619		0.4354	0.385	0.4047	0.4626	0.5618	0.391
	1.3569	1.5152	1.6649	1.8106	1.4227	1.5137		0.5071	0.507	0.6548	0.6156	0.5387	0.5323
	1.3418	1.5823	1.5072	1.5856	1.2951	1.5251		0.5026	0.567	0.5725	0.6471	0.5618	0.7162
	1.4258	1.6402	1.5314	1.5298	1.3893	1.5084		0.3798	0.5477	0.5139	0.4785	0.5312	0.5683
	1.5727	1.6442	1.5837	1.4779	1.4046	2.0132		0.6407	0.7297	0.7993	0.6673	0.7725	0.7409
Average Absorbance Values	1.48968	1.53044	1.57186	1.58976	1.38762	1.60446		0.49312	0.54728	0.58904	0.57422	0.5932	0.58974
% of control (0 J/cm^2)	100	102.7362	105.5166	106.7182	93.14886	107.705		33.10241	36.73809	39.54138	38.54653	39.82063	39.58837

(B) LLLT on MCF-7 cells without and with cisplatin at IC_{50} (17 μM)

	without Cisplatin							with Cisplatin (17 uM)					
Energy Density (J/cm^2)	0	0.1	0.5	1	3	10		0	0.1	0.5	1	3	10
Absorbance Values	1.7344	1.7506	1.7545	1.8128	1.7313	1.9252		0.7309	0.7829	0.6893	0.7623	0.9782	0.8637
	1.764	1.7166	1.8857	1.781	1.8819	1.8757		0.826	0.7651	0.7559	0.7973	0.8764	0.9484
	1.8487	1.7609	1.7256	1.7728	1.8358	1.6401		0.7381	0.8123	0.7952	0.8649	0.8487	0.8067
	1.8386	1.8121	1.8044	1.8508	1.7713	1.7087		0.928	0.9581	0.8894	0.8489	0.9719	0.8513
	1.9591	1.9077	1.8369	1.7743	1.759	1.819		0.8607	0.7764	0.8841	1.0374	0.8216	0.9219
Average Absorbance Values	1.82896	1.78958	1.80142	1.79834	1.79586	1.79374		0.81674	0.81896	0.80278	0.86216	0.89936	0.8784
% of control (0 J/cm^2)	100	97.84686	98.49423	98.32582	98.19023	98.07432		44.65597935	44.77736	43.8927	47.13936	49.1733	48.02729

(C) LLLT on Jurkat E6-1 cells without and with 5-FU at IC_{50} (20 µM)

	without 5-FU							with 5-FU (20 uM)					
Energy Density (J/cm^2)	0	0.1	0.5	1	3	10		0	0.1	0.5	1	3	10
Absorbance Values	0.4169	0.4507	0.3981	0.397	0.4042	0.4222		0.2049	0.2224	0.2082	0.2071	0.2084	0.2005
	0.4234	0.4371	0.4389	0.4323	0.4232	0.4518		0.209	0.219	0.2217	0.2079	0.2159	0.2116
	0.415	0.444	0.4206	0.4198	0.4727	0.4563		0.2303	0.2326	0.2272	0.2232	0.2235	0.2092
	0.434	0.4193	0.4426	0.3972	0.4278	0.4418		0.2208	0.2165	0.2266	0.2137	0.201	0.2106
Average Absorbance Values	0.422325	0.437775	0.42505	0.411575	0.431975	0.443025		0.21625	0.222625	0.220925	0.212975	0.2122	0.207975
% of control (0 J/cm^2)	100	103.6583	100.6452	97.45457	102.285	104.9014		51.20464098	52.71414	52.31161	50.42917	50.24566	49.24525

(D) LLLT on Jurkat E6-1 cells without and with cisplatin at IC_{50} (7 µM)

	without cisplatin							with cisplatin (7 uM)					
Energy Density (J/cm^2)	0	0.1	0.5	1	3	10		0	0.1	0.5	1	3	10
Absorbance Values	0.4016	0.4262	0.3998	0.4067	0.3911	0.4465		0.1368	0.1411	0.1467	0.1392	0.1425	0.1431
	0.3825	0.4097	0.4197	0.3837	0.4054	0.4064		0.1316	0.1415	0.1369	0.1457	0.1382	0.1446
	0.4106	0.3885	0.4129	0.3912	0.4059	0.3935		0.1388	0.1418	0.1413	0.1461	0.1433	0.146
	0.4098	0.3993	0.3951	0.4296	0.4244	0.4475		0.1441	0.1414	0.1428	0.1474	0.1483	0.1533
Average Absorbance Values	0.401125	0.405925	0.406875	0.4028	0.4067	0.423475		0.137825	0.14145	0.141925	0.1446	0.143075	0.14675
% of control (0 J/cm^2)	100	101.1966	101.4335	100.4176	101.3898	105.5718		34.35961359	35.26332	35.38174	36.04861	35.66843	36.58461

REFERENCES

Abergel, R. P., Lyons, R. F., Castel, J. C., Dwyer, R. M., & Uitto, J. (1987). Biostimulation of wound healing by lasers: experimental approaches in animal models and in fibroblast cultures. *Journal of Dermatologic Surgery and Oncology*, 13(2), 127–33.

Artyukhov, V. G., Basharina, O. V., Pantak, A. A., & Sveklo, L. S. (2000). Effect of helium-neon laser on activity and optical properties of catalase. *Bulletin of Experimental Biology and Medicine*, 129(6), 537–540.

Avci, P., Gupta, A., Sadasivam, M., Vecchio, D., Pam, Z., Pam, N., & Hamblin, M. R. (2013). Low-Level Laser (Light) Therapy (LLLT) in Skin: Stimulating, Healing, Restoring. *Seminars in Cutaneous Medicine and Surgery*, 32(1), 41–52.

Barolet, D., Roberge, C. J., Auger, F. A., Boucher, A., & Germain, L. (2009). Regulation of skin collagen metabolism in vitro using a pulsed 660 nm LED light source: clinical correlation with a single-blinded study. *Journal of Investigative Dermatology*, 129(12), 2751–9.

Ben-Dov, N., Shefer, G., Irintchev, A., Wernig, A., Oron, U., & Halevy, O. (1999). Low-energy laser irradiation affects satellite cell proliferation and differentiation in vitro. *Biochimica et Biophysica Acta*, 1448(3), 372–80.

Chung, H., Dai, T., Sharma, S. K., Huang, Y. Y., Carroll, J. D., & Hamblin, M. R. (2012). The nuts and bolts of low-level laser (light) therapy. *Annals of Biomedical Engineering*, 40(2), 516–33.

de C. Monteiro, J. S., Pinheiro, A. L., de Oliveira, S. C., Aciole, G. T., Sousa, J. A., Cangussu, M. C., & dos Santos, J. N. (2011). Influence of Laser Phototherapy (λ660 nm) on the Outcome of Oral Chemical Carcinogenesis on the Hamster Cheek Pouch Model: Histological Study. *Photomedicine and Laser Surgery*, 29(11), 741–745.

Dojindo Molecular Technologies, Inc. (2013, 9 18). *Cell Counting Kit-8: Technical Manual: Dojindo.* Retrieved from Dojindo: http://www.dojindo.com/TechnicalManual/Manual_CK04.pdf

El Batanouny, M., Korraa, S., & Fekry, O. (2002). Mitogenic potential inducible by He:Ne laser in human lymphocytes in vitro. *Journal of Photochemistry and Photobiology B: Biology*, 68(1), 1–7.

Guzzardella, G. A., Fini, M., Torricelli, P., Giavaresi, G., & Giardino, R. (2002). Laser stimulation on bone defect healing: an in vitro study. *Laser in Medical Science*, 17(3), 216–20.

Hamblin, M. R. (2008, 8 14). *Mechamisms of low level light therapy*. Retrieved from Photobiology: http://www.photobiology.info/Hamblin.html#TOP

Huang, Y.-Y., Hamblin, M., & Chen, A. C.-H. (2009, July 9). *Low-level laser therapy: an emerging clinical paradigm*. Retrieved from SPIE: http://spie.org/newsroom/technical-articles-archive/1669-low-level-laser-therapy-an-emerging-clinical-paradigm

Moore, P., Ridgway, T. D., Higbee, R. G., Howard, E. W., & Lucroy, M. D. (2005). Effect of wavelength on low-intensity laser irradiation-stimulated cell proliferation in vitro. *Lasers in Surgery and Medicine*, 36(1), 8–12.

multichromatic, sunlight, monochromatic and coherent light. (2011, February 22). Retrieved from The Science of Acne: http://thescienceofacne.com/ipl/multichromatic-sunlight-monochromatic-and-coherent-light/

Myakishev-Rempel, M., Stadler, I., Brondon, P., Axe, D. R., Friedman, M., Nardia, F. B., & Lanzafame, R. (2012). A Preliminary Study of the Safety of Red Light. *Photomedicine and Laser Surgery*, 30(9), 551–558.

Pastore, D., Greco, M., & Passarella, S. (2000). Specific helium-neon laser sensitivity of the purified cytochrome c oxidase. *International Journal of Radiation Biology*, 76(6), 863–870.

Pinheiro, A. L., Do Nascimento, S. C., Vieira, A. L., Rolim, A. B., Da Silva, P. S., & Brugnera, A. (2002). Does LLLT Stimulate Laryngeal Carcinoma Cells? *Brazilian Dental Journal*, 13(2), 109–112.

Schindl, A., Heinze, G., Schindl, M., Pernerstorfer-Schon, H., & Schindl, L. (2002). Systemic Effects of Low-Intensity Laser Irradiation on Skin Microcirculation in Patients with Diabetic Microangiopathy. *Microvascular Research*, 64(2), 240–246.

Siddik, Z. H. (2003). Cisplatin: mode of cytotoxic action and molecular basis of resistance. *Oncogene*, 22(47), 7265–79.

Sigma-Aldrich. (n.d.). *5-Fluorouracil: Sigma-Aldrich*. Retrieved from Sigma-Aldrich: http://www.sigmaaldrich.com/catalog/product/sigma/f6627?lang=en&region=US

Tuby, H., Maltz, L., & Oron, U. (2006). Modulations of VEGF and iNOS in the rat heart by low level laser therapy are associated with cardioprotection and enhanced angiogenesis. *Lasers in Surgery and Medicine*, 38(7), 682–8.

What is LLLT? - THOR Laser. (2015). Retrieved from THOR Laser: http://www.thorlaser.com/LLLT/

Yu, W., Naim, J., & Lanzafame, R. J. (1994). The effect of laser irradiation on the release of bFGF from 3T3 fibroblasts. *Photochemistry and Photobiology*, 59(2), 167–70.

Zhang, Y., Song, S., Fong, C. C., Tsang, C. H., Yang, Z., & Yang, M. (2003). cDNA microarray analysis of gene expression profiles in human fibroblast cells irradiated with red light. *Journal of Investigative Dermatology*, 120(5), 849–57.

Zigmond, E., Varol, C., Kaplan, M., Shapira, O., & Melzer, E. (2014). Low-Level Light Therapy Induces Mucosal Healing. *Photomedicine and Laser Surgery*, 32(8), 450–457.

VITA

ANDREW S. JEONG

5 Greenwood St, Wakefield, MA 01880
(801) 502-4538, ajeong28@gmail.com

Year of Birth: 1987

Education

Boston University School of Medicine, Boston, MA, Present
Candidate for Master of Arts in Medical Sciences
Expected to graduate in May, 2016

The Johns Hopkins University, Baltimore, MD, 2010
Bachelor of Arts in Chemistry

Research Experience

Safety Evaluation of Low-Level Light Therapy on Cancer Cells (Master's Thesis)
Wellman Center for Photomedicine at the Massachusetts General Hospital, Boston, MA, Present

- Determined the half-maximal inhibitory concentration (IC_{50}) of 5-fluorouracil (5-FU) and cisplatin in MCF-7 cells
- Determined the IC_{50} of 5-FU and cisplatin in Jurkat E6-1 cells
- Determined the viability of MCF-7 cells after the application of low level light in the absence and the presence of 5-FU and cisplatin at its IC_{50}
- Determined the viability of Jurkat E6-1 cells after the application of low level light in the absence and the presence of 5-FU and cisplatin at its IC_{50}

Laboratory Technician
Pediatrics Department of Johns Hopkins Medicine, Baltimore, MD, 2010 – 2011

- Examined the timing of puberty and the first estrus of ovary-specific insulin receptor knockout (OIRKO) mice through vaginal opening and vaginal smearing respectively
- Scrutinized the estrous cycle of diet-induced obese female mice using OIRKO and wild type mice through administration of hi-fat diet and vaginal smearing
- Examined the estrous cycle of female wild type mice under regular diet
- Tested mRNA expression of gonadotropin releasing hormone (GnRH) under treatment of ciliary neurotrophic factor using GnRH-secreting neuronal cell line
- Genotyped tissue-specific knockout mice through collection of tail, extraction of DNA, conducting polymerase chain reaction, and running gel-electrophoresis

- Organized and maintained wild type and unique mouse models of metabolic disorders by taking responsibilities in breeding, mating, and weaning

Research and Reading in Gastrointestinal (GI) System (Received academic credits)
Gastroenterology Department of Johns Hopkins Medicine**,** Baltimore**,** MD, Spring of 2010

- Scrutinized molecular mechanisms of microbial infections of epithelial cells through functional analysis of effectors, scaffolding proteins, membrane channels & pumps (Sodium-hydrogen antiporter in particular), and intracellular signaling proteins
- Presented an article "The enteropathogenic *Escherichia coli* type 3 secretion system effector Map binds EBP50/NHERF1: implication for cell signaling and diarrhea"
- Read scientific journals of cell & molecular biology relevant to GI pathologies, and attended seminars and presentations of journal club

A comparison study of the Visual-Memory Stimulating (VMS) grid and the Amsler grid as self-monitoring tools for patients with Age-related Macular Degeneration (Received academic credits)
Wilmer Eye Institute at Johns Hopkins Medicine, Baltimore, MD, 2008 – 2009

- Recruited and tested patients with the VMS grid and the Amsler grid
- Recorded data and responses noted by patients
- Conducted quantitative and qualitative analyses on effectiveness of both grids in detecting the areas of visual distortions
- Analyzed preferences specified by patients in terms of ease, accuracy, and confidence
- Validated against retinal imaging results

Teaching Experience

English Teacher
Top Language Tutoring**,** Jeonju, South Korea, Summer of 2007

- Taught English to Korean elementary school students

Mathematics Tutor
Top Language Tutoring**,** Jeonju, South Korea, Summer of 2007

- Taught elementary & intermediate algebra to Korean middle school students

Clinical Experience

Unite For Sight Global Impact Fellow (Volunteer)
Accra and Kumasi region of Ghana, Summer of 2011

- Fund-raised to provide patient care and free surgeries to those who are in extreme poverty

- Participated in daily outreach programs organized by eye clinics to assist in on-site patient care
- Registered patients for eye exam, conducted visual acuity screening, distributed medication and glasses, educated patients about basic preventative measures, and observed eye surgeries

Volunteer/Shadower
Wilmer Eye Clinic at Johns Hopkins Hospital, Baltimore, MD, Apr 2011

- Assisted in visual acuity screening, and observed eye care provided by an ophthalmologist

Projects Abroad Medical Internship Volunteer/Shadower
Gastroenterology/Ophthalmology department of Ruijin Hospital, Shanghai, China, Summer of 2010

- Observed surgeries and patient care relevant to ophthalmic and GI conditions

Volunteer/Shadower
Pediatric department of Sinai Hospital, Baltimore, MD, Jun 2010

- Observed pediatric care in anesthesia, MRI, blood work, and dental treatment

Volunteer/Shadower
Wilmer Eye Clinic at Wyman Park of Johns Hopkins Hospital, Baltimore, MD, Summer of 2008

- Assisted in patient flow
- Observed eye exams and patient care relevant to eye conditions provided by an optometrist

Professional Memberships and Honors

The American Chemical Society, 2010
Dean's List, 2008
Carl A. Knierim Scholar, 2008

Poster

R. Gulati, M. Roser, S. Torr-Brown, A. Jeong, G. Dagnelie; A Comparison Study of the Visual & Memory Stimulating (VMS) Grid and the Amsler grid as Self-monitoring tools for Age-related Macular Degeneration, 2009

Conference

The Association for Research in Vision and Ophthalmology (ARVO) 2009 Annual Conference, Fort Lauderdale, FL, May 3–7, 2009

Foreign Language

Fluent in Korean